Three-dimensional fracton topological orders with boundary Toeplitz braiding

Boxi Li,* Yao Zhou,* and Peng Ye[†]
Guangdong Provincial Key Laboratory of Magnetoelectric Physics and Devices,
State Key Laboratory of Optoelectronic Materials and Technologies,
and School of Physics, Sun Yat-sen University, Guangzhou, 510275, China
(Dated: Tuesday 23rd July, 2024)

In this paper, we theoretically study a class of 3D non-liquid states that show exotic boundary phenomena in the thermodynamical limit. More concretely, we focus on a class of 3D fracton topological orders formed via stacking 2D twisted \mathbb{Z}_N topologically ordered layers along z-direction. Nearby layers are coupled while maintaining translation symmetry along z direction. The effective field theory is given by infinite-component Chern-Simons theory, with an integer-valued symmetric block-tridiagonal Toeplitz K-matrix whose size is thermodynamically large. With open boundary conditions (OBC) along z, certain choice of K-matrices exhibits exotic boundary "Toeplitz braiding", where the mutual braiding phase angle between two anyons at opposite boundaries oscillates and remains non-zero in the thermodynamic limit. In contrast, in trivial case, the mutual braiding phase angle decays exponentially to zero in the thermodynamical limit. As a necessary condition, this phenomenon requires the existence of boundary zero modes in the K-matrix spectrum under OBC. We categorize nontrivial K-matrices into two distinct types. Each type-I possesses two boundary zero modes, whereas each type-II possesses only one boundary zero mode. Interestingly, the integer-valued Hamiltonian matrix of the familiar 1D "Su-Schrieffer-Heeger model" can be used as a non-trivial K-matrix. Importantly, since largegauge-invariance ensures integer quantized K-matrix entries, global symmetries are not needed to protect these zero modes. We also present numerical simulation as well as finite size scaling, further confirming the above analytical results. Motivated by the present field-theoretical work, it will be interesting to construct 3D lattice models for demonstrating Toeplitz braiding, which is left to future investigation.

I. INTRODUCTION

Recently, research on topologically-ordered non-liquid states [1] has flourished, notably fracton topological order (FTO) [2]. These strongly-correlated systems with long-range entanglement have point-like excitations with limited mobility, unlike conventional intrinsic topological orders where excitations move freely without extra energy cost. FTOs' sensitivity to lattice details prevents a conventional continuum limit, setting them apart from liquid states. Exactly solvable models like the X-cube model [3] and Haah's code [4] reveal these properties. A large class of FTO models, including the X-cube model, display a foliation structure, showing that some $(3+1)D^1$ FTOs can be seen as stacks of coupled (2+1)D topological orders. From the entanglement perspective, extracting layers of (2+1)D topological orders resembles "coarse graining" within the entanglement renormalization group framework. Here, the X-cube model is the fixed point of entanglement renormalization [5], and the entanglement renormalization group provides a hierarchical structure [6] for various topologically-ordered non-liquid states [7, 8].

As the analysis of lattice models indicates that many FTOs can be constructed by properly stacking and coupling lower-dimensional topologically-ordered liquid states. This prompts the question of what the field-theoretic counterpart is for the process of stacking topological orders. Along this line of thinking, one solution is to take full use of so-called infinite-component Chern-Simons theory (iCS), which is a very useful

and powerful (3+1)D field theory recently studied in Refs. [9–14]. Let us elaborate more.

It is known that the effective theories of (2+1)D Abelian topological orders are K-matrix Chern-Simons theories [15], which provide a framework to understand a large class of topologically-ordered states, including multilayer fractional quantum Hall effects, spin liquids, and others. They also offer a systematic platform to classify symmetry-enriched topological (SET) and symmetry-protected topological (SPT) phases in (2+1)D, see, e.g., Refs. [16–22]. In the following, we assume all these (2+1)D topological orders reside in the spacetime with coordinates parameterized by x, y, t. So, the wavefunctions of these states are defined on an xy plane. Next, one can stack each (2+1)D theory one by one along z direction in order to form a multilayer quantum state. If the layer number tends to infinity, one ends up with an authentic (3+1)D quantum state. For example, one can start with the Laughlin state described by the Chern-Simons theory $\mathcal{L} = \frac{m}{4\pi} a_{\mu} \partial_{\nu} a_{\lambda} \epsilon^{\mu\nu\lambda}$, where a_{μ} is a U(1) gauge field and $m \in \mathbb{Z}$. By stacking the Laughlin states and coupling the nearby layers, we obtain the effective theory for (3+1)D fractional quantum Hall states. The transport properties of the lateral surfaces of these states have been widely studied both theoretically and experimentally [23–28]. The resulting low-energy effective theory of a multilayer fractional quantum Hall state is a multi-component Chern-Simons (mCS) theory, described by the Lagrangian $\mathcal{L} = \sum_{I=1}^N \frac{m}{4\pi} a_\mu^I \partial_\nu a_\lambda^I \epsilon^{\mu\nu\lambda}$, where N refers to the number of layers. In this context, the superscript I, originally defined as the layer index, represents the location of the gauge field along z direction. If N is pushed to infinity, the resulting theory is an aforementioned infinite-component Chern-Simons, i.e., iCS field theory.

In this paper, we focus on iCS field theories in which each layer is a *twisted* \mathbb{Z}_m *topological or-*

^{*} These authors contributed equally to this work.

[†] yepeng5@mail.sysu.edu.cn

¹ In this paper, "n + 1D" refers to (n + 1)-dimensional spacetime, while "nD" refers to n spatial dimensions.

der described by a two-component Chern-Simons theory $\frac{1}{4\pi}\sum_{I,J=1}^{2}\mathcal{K}_{IJ}a_{\mu}^{I}\partial_{\nu}a_{\lambda}^{J}\epsilon^{\mu\nu\lambda}$. Here, $\mathcal{K}=\begin{pmatrix}n&m\\m&0\end{pmatrix}$ with $m,n\in\mathbb{Z}$. a_{μ}^{I} is a compact U(1) gauge field restricted on the I-th layer, meaning that I may serve as the coordinate along z direction (assuming that each layer is on xy plane). After stacking these (2+1)D twisted topological orders and coupling the nearby layers by additional Chern-Simons terms (see Fig. 1a), we can find that the K-matrix of the resulting iCS field theory is a block-tridiagonal Toeplitz matrix (to be shown in Eq. (2) in Sec. II). Locality of the resulting 3D theory requires that K_{IJ} must decay no slower than exponential decay as |I-J| increases. For the sake of simplicity, we only consider the coupling between nearest (2+1)D topological orders.

Mathematically, Toeplitz matrices are defined as matrices possessing translation symmetry along each diagonal. They find wide applications in both physics and mathematics [29– 35]. When individual entries of a Toeplitz matrix are replaced by matrix blocks, the resulting matrix is referred to as a block Toeplitz matrix. Interestingly, the formalism of the block-tridiagonal Toeplitz matrix immediately reminds us of a single-particle Hamiltonian of a 1D tight-binding lattice fermion model. Research on topological insulators (TIs) and topological superconductors (TSCs) has shed light on some Toeplitz matrices possessing eigenvectors localized at boundaries [36–41] when open boundary condition (OBC) is imposed. These eigenvectors have eigenvalues that decrease exponentially to zero as the size of the matrix increases, which is well-known as boundary zero modes in the thermodynamical limit. We must stress that, such an analogy is made only on the level of similar mathematics. It is important to note that Kmatrix here is not a Hamiltonian, and all matrix elements here are strictly quantized to integers due to large gauge invariance. As is known from the study of TIs and TSCs, boundary zero modes contain rich topological physics. Inspired by research in TIs and TSCs, we wonder whether and how the potential presence of boundary zero modes of the matrix K reshape the low-lying energy physics of (3+1)D fracton topological order described by iCS field theory. Especially, in the presence of boundary zero modes of K-matrices, do there exist nontrivial properties on z-boundaries (i.e., two boundaries along z direction) of iCS field theory?

In this paper, we investigate these questions through certain iCS field theories under OBC in the z-direction (denoted as z-OBC). Specifically, we couple twisted \mathbb{Z}_m topological orders layer-by-layer, which leads to K-matrices that take the form of block Toeplitz matrices. It should be noted that, again, the "boundary zero modes" of Toeplitz K-matrices discussed here are not physical edge modes of TIs. Instead, they are, in a pure mathematical sense, eigenvalues of dimensionless K-matrices with OBC, which decrease exponentially to zero as the size of the K-matrix, i.e., the number of layers N, increases from finite to infinite. Due to the presence of boundary zero modes in the K-matrix, we observe that the

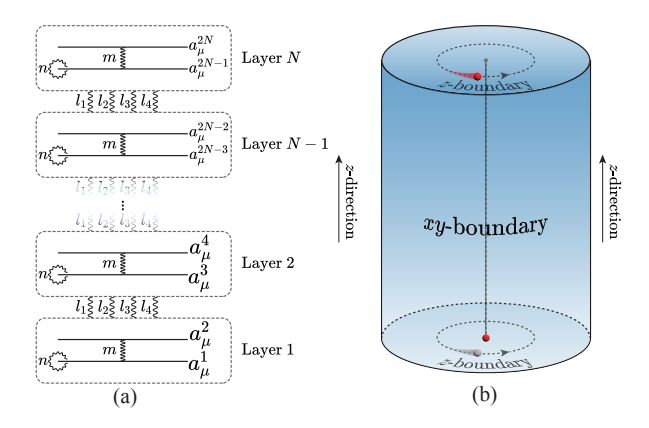


FIG. 1. (a) is an illustrative diagram of stacking \mathbb{Z}_m twisted topological orders. After stacking these \mathbb{Z}_m twisted topological orders, we obtain a 3-dimensional theory as illustrated in (b). In the following discussion, open boundary condition is applied in z-direction. In our discussion, we focus on the asymptotic behaviour as the number of layer N goes to infinity. (b) is also an illustrative diagram of braiding process between excitations residing at distinct z-boundaries. The topological excitations are plotted as red dots in (b). If the K-matrix of the iCS field theory has boundary zero mode, together with the condition that the upper-right and lower-left entries of K^{-1} are non-integers, two topological excitations residing at distinct z-boundaries can be detected mutually via mutual braiding (i.e., Toeplitz braiding) in the thermodynamical limit.

braiding statistics between topological excitations, even when widely separated along the z direction, may be nontrivial, except for some very special cases. As an extreme example, Fig. 1(b) illustrates the braiding process between topological excitations residing at distinct z-boundaries, which also clarifies how the braiding of two excitations is practically performed. In this paper, this mutual braiding statistics is termed "Toeplitz braiding" in order to highlight the nontrivial mathematical properties of Toeplitz matrices.

More analytically, we find that the presence of Toeplitz braiding necessitates not only the existence of boundary zero modes of K-matrices but also non-integer values of the upperright and lower-left components of K^{-1} (to be shown in Fig. 4(b) in the main text). We classify K-matrices that potentially support Toeplitz braiding into two distinct types and numerically verify how the braiding phase angle constantly oscillates as the number of layers along the z direction tends to infinity. To make a clear comparison, we also numerically compute a trivial case, where the mutual braiding phase angle exponentially decays to zero in the thermodynamical limit. By taking full advantage of the properties of Toeplitz matrices and making a tight connection to the calculation of braiding statistics of Chern-Simons gauge theory, our work presented here illuminates the exotic boundary topological physics of 3D strongly-correlated states, advancing the exploration of topologically ordered non-liquids including fracton topological orders. Several interesting future directions are straightforward.

The paper is organized as follows. In Sec. II, we carry on an analytic analysis on a concrete iCS field theory with Toeplitz

 $^{^2}$ In the following text, the term "K-matrix" primarily refers to the Toeplitz K-matrix, as represented by Eq. (2), unless explicitly stated otherwise.

braiding, whose K-matrix is, in its mathematical form, equivalent to the Hamiltonian of Su-Schrieffer-Heeger model [36]. In Sec. III, we propose a general framework for sorting K-matrices with boundary zero modes. Within this framework, we identify two distinct types of K-matrices that possess boundary zero modes, providing them as illustrative examples. The results are shown in Table I. To demonstrate the correspondence between boundary zero modes of K-matrices and nonlocal braiding statistics in z-direction in these models, we conduct numerical computations in Sec. IV. This work is concluded in Sec. V.

II. CONSTRUCTION OF ICS FIELD THEORY AND TOEPLITZ BRAIDING

A. iCS field theory with twisted \mathbb{Z}_m topologically ordered layers

The construction of an iCS field theory can be regarded as the process of stacking \mathbb{Z}_m topological orders. We initiate our analysis from the \mathbb{Z}_m twisted topological order, which is described by the K-matrix Chern-Simons theory $\mathcal{L} = \frac{1}{4\pi} \sum_{I,J} A_{IJ} a^I_\mu \partial_\nu a^J_\lambda \epsilon^{\mu\nu\lambda}$. Here, A is specified as $A = \begin{pmatrix} n & m \\ m & 0 \end{pmatrix}$. Here, a^I_μ is a U(1) gauge field and n,m are quantized to integers due to the invariance under large gauge transformations. Given a stack of \mathbb{Z}_m twisted topological order, we add Chern-Simons terms to couple the nearby layers, which corresponds to the off-diagonal blocks in the K-matrix. The stacking direction is dubbed the z-direction hereafter, and the resulting theory is described by the following Lagrangian:

$$\mathcal{L} = \frac{1}{4\pi} \sum_{I,J} K_{IJ} a^I_\mu \partial_\nu a^J_\lambda \epsilon^{\mu\nu\lambda},\tag{1}$$

where

$$K = \begin{pmatrix} A & B^{T} & & & & \\ B & A & B^{T} & & & & \\ & B & A & B^{T} & & & \\ & & \ddots & \ddots & \ddots & \\ & & & B & A & B^{T} \\ & & & & B & A \end{pmatrix}, \tag{2}$$

with $A=\begin{pmatrix}n&m\\m&0\end{pmatrix}$ and $B=\begin{pmatrix}l_1&l_2\\l_3&l_4\end{pmatrix}$, as shown in Eq. (2). Fig. 1(a) gives an illustration of the stacking process. Each layer is a \mathbb{Z}_m twisted topological order described by K-matrix Chern-Simons theory corresponding to diagonal blocks A in the Toeplitz K-matrix. The nearby layers are coupled by Chern-Simons terms, which corresponds to the upper-right and lower-left 2×2 blocks B in the K-matrix. For example, Layer 1 contributes intra-layer Chern-Simons terms $\frac{1}{4\pi}[m(a_\mu^1\partial_\nu a_\lambda^2+a_\mu^2\partial_\nu a_\lambda^1)+n(a_\mu^1\partial_\nu a_\lambda^1)]\epsilon^{\mu\nu\lambda}$. The inter-layer Chern-Simons terms between Layer 1 and Layer 2 are $\frac{1}{4\pi}[l_1(a_\mu^1\partial_\nu a_\lambda^3+a_\mu^3\partial_\nu a_\lambda^1)+l_2(a_\mu^3\partial_\nu a_\lambda^2+a_\mu^2\partial_\nu a_\lambda^3)+l_3(a_\mu^4\partial_\nu a_\lambda^1+a_\mu^1\partial_\nu a_\lambda^4)+l_4(a_\mu^4\partial_\nu a_\lambda^2+a_\mu^2\partial_\nu a_\lambda^4)]\epsilon^{\mu\nu\lambda}$. If we

stack N layers of twisted \mathbb{Z}_m topological order, the resulting theory is a multi-component Chern-Simons theory with a 2N-dimensional K-matrix. As the number of layers N goes to infinity, the mCS theory becomes an iCS field theory as illustrated in Fig. 1(b). All the coefficients in the K-matrix are integers due to large gauge invariance. In this setting, the superscript I of a gauge field a_μ^I carries the meaning of the z-coordinate. The I-th layer contains two independent gauge fields a_μ^{2I-1} and a_μ^{2I} . We should be extremely careful about the general basis transformation $K \to W^T KW$, $W \in GL(2N,\mathbb{Z})$, requiring it to preserve the locality in the z-direction. The absence of upper-right and lower-left blocks indicates that we are discussing iCS field theories in z-OBC.

To discuss the braiding statistics between topological excitations, excitation terms need to be included in the Lagrangian Eq. (1). In K-matrix Chern-Simons theories, topological excitations are labeled by integer vectors $\mathbf{p} = (p^1, p^2, \dots, p^{2N})^T, \mathbf{q} = (q^1, q^2, \dots, q^{2N})^T, \dots \in \mathbb{Z}^{2N}$, and the excitation terms corresponding to \mathbf{p} and \mathbf{q} are given by $p^I a^I_{\mu} j^\mu_{\mathbf{p}}$ and $q^I a^I_{\mu} j^\mu_{\mathbf{q}}$, respectively, where $j^\mu_{\mathbf{p}}$ and $j^\mu_{\mathbf{q}}$ are the currents of topological excitations. After integrating out the gauge fields, the mutual braiding phase angle between topological excitations \mathbf{p} and \mathbf{q} is given by

$$\Theta_{\mathbf{p},\mathbf{q}} = 2\pi p^I (K^{-1})_{IJ} q^J, \mod 2\pi. \tag{3}$$

This paper imposes a restriction on the mutual braiding phase angle, limiting it to the interval $[-\pi, \pi)$ unless otherwise specified. In the following text, we use l_I , $I \in 1, ..., 2N$ to label the topological excitation carrying unit gauge charge, coupled to gauge field a_{μ}^{I} . For example, $\mathbf{l}_{1}=(1,0,\ldots,0)^{T}$ labels an excitation coupled to the a^1_μ gauge field, residing at a z-boundary, while $\mathbf{l}_{2N} = (0, \dots, 0, 1)^T$ labels an excitation residing at another z-boundary, coupled to gauge field $a_{\mu}^{2N}.$ The mutual braiding phase angle between \mathbf{l}_1 and \mathbf{l}_{2N} is $\Theta_{\mathbf{l}_1,\mathbf{l}_{2N}}=2\pi(K^{-1})_{1,2N}\mod 2\pi.$ This example also tells us that the lower-left and upper-right elements of K^{-1} describe the braiding phase angle between excitations residing at distinct z-boundaries, as illustrated in Fig. 2(a). On the contrary, the diagonal elements of K^{-1} characterize the braiding statistics of excitations, where the distance between them is finite along the z-direction, as illustrated in Fig. 2(b).

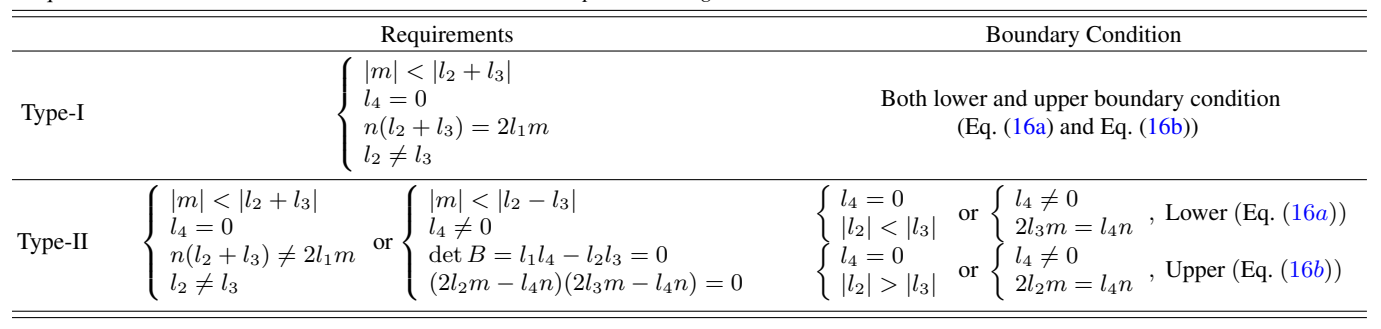
B. Boundary zero modes and Toeplitz braiding: A concrete example

Zero modes of K-matrices have the following properties: for a finite size K-matrix, the zero modes have finite values instead of being zero. As the size of the system, i.e., the size of the K-matrix, increases, the eigenvalues decrease to zero exponentially. Therefore, for a finite size K-matrix, the inverse K^{-1} is always well-defined. In the following discussion, we mainly focus on the asymptotic behavior of K^{-1} as

 $^{^3}$ In this paper, taking thermodynamical limit refers to taking the limit $N \to \infty$ along z-direction. Each xy layer is already in the thermodynamical limit.

TABLE I. A class of Toeplitz K-matrices (Eq. (2)) with boundary zero modes, where the block $A = \begin{pmatrix} n & m \\ m & 0 \end{pmatrix}$ and the block $B = \begin{pmatrix} l_1 & l_2 \\ l_3 & l_4 \end{pmatrix}$. Type-I K-matrix possesses 2 boundary zero mode, whereas Type-II K-matrix possesses 1 boundary zero modes. It should be noted that the

"requirement" column is not the sufficient condition for Toeplitz braiding.



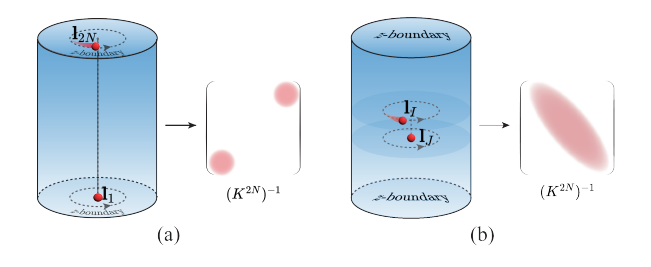


FIG. 2. (a) is an illustrative diagram of braiding process between topological excitations residing at distinct z-boundaries. In general, upper-right and lower-left elements of matrix $(K^{2N})^{-1}$ describe the braiding statistics. (b) is an illustrative diagram of braiding process between topological excitations l_I and l_J that are close in zcoordinates ($|I-J| \ll 2N$), which is described by the diagonal elements of matrix $(K^{2N})^{-1}$.

the number of layers $N \to \infty$. Thus, practically, the inverse of K is calculated before taking the limit of the system size⁴ $2N \to \infty$.

To gain insights, we focus on a simple example, where the Lagrangian is given by Eq. (1), and the K-matrix (denoted as K_1 -matrix hereafter) is given by Eq. (2). The A and B blocks read:

$$A = \begin{pmatrix} 0 & m \\ m & 0 \end{pmatrix}, \quad B = \begin{pmatrix} 0 & l \\ 0 & 0 \end{pmatrix}, \tag{4}$$

where $m, l \in \mathbb{Z}$. Denote the K-matrix of size 2N with block A, B given by Eq. (4) as K_1^{2N} , which is, in its mathematical form, equivalent to the Hamiltonian of Su-Schrieffer-Heeger

model. The inverse $(K_1^{2N})^{-1}$ reads [42]

$$(K_1^{2N})^{-1} = \begin{pmatrix} 0 & \frac{1}{m} & 0 & -\frac{1}{m^2} & 0 & \cdots & 0 & \frac{1}{m}(-\frac{1}{m})^{N-1} \\ \frac{1}{m} & 0 & 0 & 0 & 0 & \cdots & 0 & 0 \\ 0 & 0 & 0 & \frac{1}{m} & 0 & \cdots & 0 & \frac{1}{m}(-\frac{1}{m})^{N-2} \\ -\frac{1}{m^2} & 0 & \frac{1}{m} & 0 & 0 & \cdots & 0 & 0 \\ \vdots & \vdots & \vdots & \vdots & \vdots & \ddots & \vdots & \vdots \\ 0 & 0 & 0 & 0 & 0 & 0 & \cdots & 0 & 0 & \frac{1}{m} \\ \frac{1}{2}(-\frac{1}{m})^{N-1} & 0 & \frac{1}{2}(-\frac{1}{m})^{N-2} & 0 & \frac{1}{2}(-\frac{1}{m})^{N-3} & \cdots & \frac{1}{2} & 0 \end{pmatrix}, (5)$$

which captures the braiding statistics between topological excitations. Following the notation in Sec. II A, the topological excitation carrying unit gauge charge, coupled to gauge field a_{μ}^{I} , is labelled by

$$\mathbf{l}_I = \begin{pmatrix} \cdots & 0 & 0 & 1 & 0 & 0 & \cdots \end{pmatrix}^T. \tag{6}$$

The subscript *I* refers to the location of the nonzero entry.

In the case of |m| > |l|, the mutual braiding phase angle between \mathbf{l}_I and \mathbf{l}_J is $2\pi[(K_1^{2N})^{-1}]_{IJ}$, decaying exponentially with respect to |I-J| for I,J satisfying $I>J,\ I=2i,\ J=$ 2j-1, or J>I, J=2j, I=2i-1, $i,j\in\mathbb{Z}^+$, which means that if two excitations reside at distinct z-boundaries, they cannot be mutually detected by braiding processes. For instance, the mutual braiding phase angle between two excitations $\mathbf{l}_1 = \begin{pmatrix} 1 & 0 & \cdots & 0 \end{pmatrix}^T$ and $\mathbf{l}_{2N} = \begin{pmatrix} 0 & \cdots & 0 & 1 \end{pmatrix}^T$ is $\frac{2\pi}{m}\left(\frac{-l}{m}\right)^N \mod 2\pi$. Since |l/m| < 1, the phase angle is suppressed to zero in thermodynamical limit $2N \to \infty$ as illustrated in Fig. 3, where we take m=2, l=1 as an example. If |l| > |m|, the matrix element $[(K_1^{2N})^{-1}]_{IJ}$ increases exponentially with |I - J| for I, J satisfying I > J, I = $2i, J = 2j - 1, \text{ or } J > I, J = 2j, I = 2i - 1, i, j \in$

 \mathbb{Z}^+ . The mutual braiding phase angle $\Theta_{\mathbf{l}_1,\mathbf{l}_{2N}} = \frac{2\pi}{m} \left(\frac{-l}{m}\right)^N$ mod 2π between \mathbf{l}_1 and \mathbf{l}_{2N} is not exponentially suppressed if l_1 mod l_2 and l_3 is not exponentially suppressed if $l \mod m^2 \neq 0$, which indicates that topological excitations l_1 and l_{2N} can be remotely detected by each other in the braiding process. As the system size increases, the braiding phase angle between two excitations located at distinct z-boundaries, l_1 and l_{2N} , exhibits oscillation, as shown in Fig. 3.

Furthermore, we will demonstrate that the presence of Toeplitz braiding requires boundary zero modes. As is known,

⁴ In this paper, system size refers to the dimension of a finite-size blocktridiagonal Toeplitz K-matrix.

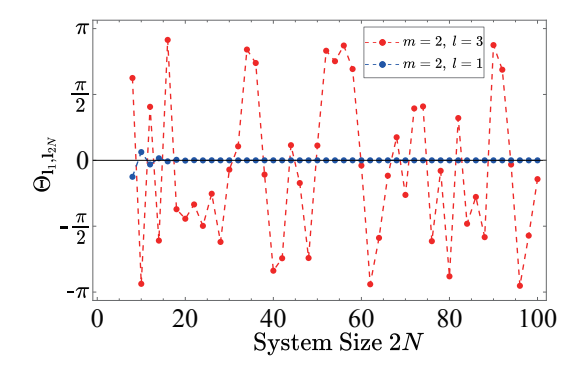


FIG. 3. The mutual braiding phase angle $\Theta_{1_1,1_{2N}}=2\pi l_1^T(K_1^{2N})^{-1}l_{2N}\mod 2\pi$, where we shift the phase angle in $(\pi,2\pi)$ to $(-\pi,0)$. If |m|>|l|, the mutual braiding phase angle $\Theta_{1_1,1_{2N}}$ is suppressed as the system size 2N increases, where we take m=2, l=1 as an example. In contrast, if |m|<|l|, the mutual braiding phase angle $\Theta_{1_1,1_{2N}}$ exhibits oscillation as the system size 2N increases. Here we take m=2, l=3 as an example.

if |l| > |m|, the K_1^{2N} matrix has boundary zero modes \mathbf{v}_1 and \mathbf{v}_2 ,

$$\mathbf{v}_1 = \frac{1}{\sqrt{2}}\mathbf{u}_1 + \frac{1}{\sqrt{2}}\mathbf{u}_2,\tag{7a}$$

$$\mathbf{v}_2 = -\frac{1}{\sqrt{2}}\mathbf{u}_1 + \frac{1}{\sqrt{2}}\mathbf{u}_2,\tag{7b}$$

where

$$\mathbf{u}_{1} = \sqrt{\frac{1 - \left(\frac{m}{l}\right)^{2}}{1 - \left(\frac{m}{l}\right)^{2N}}}$$

$$\left(1, 0, \left(-\frac{m}{l}\right), 0, \left(-\frac{m}{l}\right)^{2}, \dots, \left(-\frac{m}{l}\right)^{N-1}, 0\right)^{T},$$
(8a)

$$\mathbf{u}_{2} = \sqrt{\frac{1 - \left(\frac{m}{l}\right)^{2}}{1 - \left(\frac{m}{l}\right)^{2N}}}$$

$$\left(0, \left(-\frac{m}{l}\right)^{N-1}, 0, \left(-\frac{m}{l}\right)^{N-2}, \cdots, \left(-\frac{m}{l}\right), 0, 1\right)^{T}.$$
(8b)

Only when the system size $2N \to \infty$, the eigenvalues of boundary zero modes are strictly equal to zero. The eigenvalues of \mathbf{v}_1 and \mathbf{v}_2 are denoted as λ_1 and λ_2 , respectively.

$$\lambda_1 = m \frac{1 - \left(\frac{m}{l}\right)^2}{1 - \left(\frac{m}{l}\right)^{2N}} \left(-\frac{m}{l}\right)^{N-1},\tag{9}$$

$$\lambda_2 = -m \frac{1 - \left(\frac{m}{l}\right)^2}{1 - \left(\frac{m}{l}\right)^{2N}} \left(-\frac{m}{l}\right)^{N-1}.$$
 (10)

The inverse of K_1^{2N} can be written as

$$(K_1^{2N})^{-1} = \frac{1}{\lambda_1} \mathbf{v}_1 \mathbf{v}_1^{\dagger} + \frac{1}{\lambda_2} \mathbf{v}_2 \mathbf{v}_2^{\dagger} + \frac{1}{\lambda_3} \mathbf{v}_3 \mathbf{v}_3^{\dagger} + \cdots + \frac{1}{\lambda_{2N}} \mathbf{v}_{2N} \mathbf{v}_{2N}^{\dagger},$$

$$(11)$$

 $\mathbf{v}_3,\dots,\mathbf{v}_{2N}$ are the other eigenvectors of K_1^{2N} , and $\lambda_3,\dots,\lambda_{2N}$ are the corresponding eigenvalues. As far as $(K_1^{2N})^{-1}$ is concerned, $\frac{1}{\lambda_1}$ and $\frac{1}{\lambda_2}$ are eigenvalues of $(K_1^{2N})^{-1}$ with largest absolute values. In the thermodynamical limit $2N\to\infty$, $\frac{1}{\lambda_1}$ and $\frac{1}{\lambda_2}$ diverge. We wonder what information is captured in

$$M_1^{2N} := \frac{1}{\lambda_1} \mathbf{v}_1 \mathbf{v}_1^{\dagger} + \frac{1}{\lambda_2} \mathbf{v}_2 \mathbf{v}_2^{\dagger}. \tag{12}$$

It should be noted that the rank of M_1^{2N} is 2, thus it is not invertible. Having \mathbf{v}_1 and \mathbf{v}_2 , we are able to write down the matrix M_1

$$M_{1}^{2N} = \frac{1}{\lambda_{1}} \mathbf{v}_{1} \mathbf{v}_{1}^{\dagger} + \frac{1}{\lambda_{2}} \mathbf{v}_{2} \mathbf{v}_{2}^{\dagger} =$$

$$\begin{pmatrix} 0 & \frac{1}{m} & 0 & -\frac{l}{m^{2}} & 0 & \cdots & \frac{1}{m} \left(-\frac{l}{m}\right)^{N-2} & 0 & \frac{1}{m} \left(-\frac{l}{m}\right)^{N-1} \\ \frac{1}{m} & 0 & -\frac{1}{l} & 0 & \frac{1}{l^{2}} & \cdots & 0 & \frac{1}{m} \left(-\frac{l}{m}\right)^{N-2} & 0 \\ 0 & -\frac{1}{l} & 0 & \frac{1}{m} & 0 & \cdots & \frac{1}{m} \left(-\frac{l}{m}\right)^{N-3} & 0 & \frac{1}{m} \left(-\frac{l}{m}\right)^{N-2} \\ \vdots & \vdots & \vdots & \vdots & \vdots & \vdots & \ddots & \vdots & \vdots & \vdots \\ \frac{1}{m} \left(-\frac{l}{m}\right)^{N-2} & \frac{1}{m} \left(-\frac{l}{m}\right)^{N-3} & 0 & \frac{1}{m} \left(-\frac{l}{m}\right)^{N-3} & \cdots & 0 & -\frac{1}{l} & 0 \\ \frac{1}{m} \left(-\frac{l}{m}\right)^{N-1} & 0 & \frac{1}{m} \left(-\frac{l}{m}\right)^{N-2} & \frac{1}{m} \left(-\frac{l}{m}\right)^{N-2} & \cdots & 0 & \frac{1}{m} \left(-\frac{l}{m}\right)^{N-3} & \cdots & 0 & \frac{1}{m} \\ \frac{1}{m} \left(-\frac{l}{m}\right)^{N-1} & 0 & \frac{1}{m} \left(-\frac{l}{m}\right)^{N-2} & \frac{1}{m} \left(-\frac{l}{m}\right)^{N-3} & \cdots & 0 & \frac{1}{m} & 0 \end{pmatrix}$$

$$\tag{13}$$

The upper-right and lower-left elements $(M_1^{2N})_{IJ}=\frac{1}{m}\left(-\frac{m}{l}\right)^{(|I-J|+1)/2},\ I=2i,\ J=2j-1,\ i,j\in\mathbb{Z}^+$ are exponentially suppressed. Therefore, M_1^{2N} gives good approximation to the upper-right and lower-left elements of $(K_1^{2N})^{-1}$. In other words, M_1^{2N} captures the long-range braiding statistics in z-direction.

It is noteworthy that in some cases, the nonzero upper-right and lower-left elements may not result in nontrivial Toeplitz braiding. For example, if $l \mod m^2 = 0$, the upper-right and lower-left entries in Eq. (5) are integers, implying that excitations residing at distinct z-boundaries cannot interact by braiding. Indeed, the presence of boundary zero modes is a necessary but not sufficient condition for the appearance of *Toeplitz braiding.* We have demonstrated that the appearance of boundary zero modes in K-matrices will result in non-zero elements in the upper-right and lower-left regions of K^{-1} . However, the elements in these regions are not guaranteed to be non-integers. The K_1 -type iCS field theory with m=2, l = 4 is a typical example. The K-matrix has boundary zero modes, but nontrivial braiding statistics is completely absent except for the topological excitations residing at the same layer, as shown in Fig. 4(a). The presence of non-integers in the upper-right and lower-left regions of K^{-1} is necessary for the occurrence of Toeplitz braiding. Therefore, we propose the following condition for the existence of Toeplitz braiding: If boundary zero modes of K along with non-integer upperright and lower-left regions of K^{-1} exist, then Toeplitz braiding occurs, which is also illustrated in Fig. 4(b).

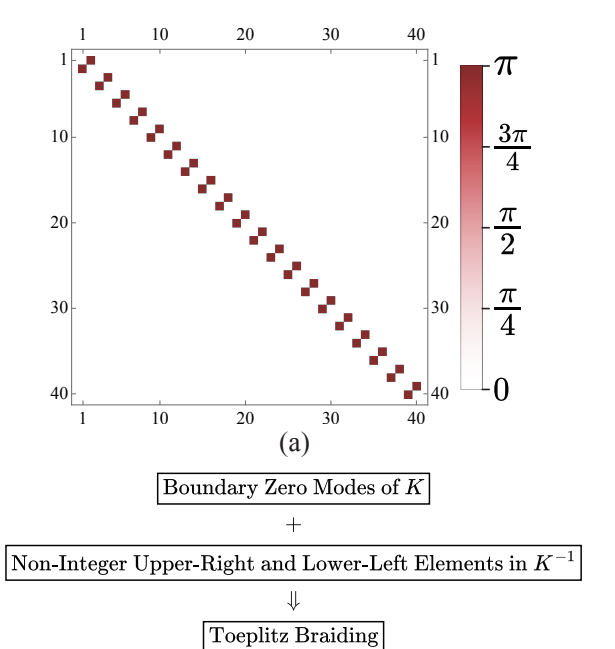


FIG. 4. (a) is the matrix plot of mutual braiding phase angle $\Theta_{1_I,1_J}=2\pi(K_1^{2N})_{IJ}^{-1}$ with m=2,l=4,2N=40, where the mutual braiding phase angle is limited to $(-\pi,\pi]$. Nontrivial braiding statistics is completely absent except for the topological excitations residing at the same layer. (b) illustrates the conditions for Toeplitz braiding.

(b)

III. SORTING K-MATRICES WITH BOUNDARY ZERO MODES

A. General approach to sorting K-matrices with boundary zero modes

Our investigation into a concrete example of iCS field theories with Toeplitz braiding in Sec. II raises an intriguing question: how to identify and classify iCS field theories with Toeplitz braiding? As illustrated in Fig. 4(b), the appearance of Toeplitz braiding demands both boundary zero modes of K and non-integer upper-right and lower-left elements in K^{-1} . In this section, we present a systematic framework for determining the presence of boundary zero modes in a given Kmatrix. As shown in Table I, we identify two different types of K-matrices with boundary zero modes as illustrative examples. The Type-I K-matrix possesses two linearly independent boundary zero modes, whereas the Type-II K-matrix exhibit only one boundary zero mode. The corresponding iCS field theories, are dubbed as Type-I and Type-II iCS field theories, respectively. The aforementioned example, an iCS field theory with an Su-Schrieffer-Heeger (SSH)-type K-matrix, represents a typical Type-I iCS field theory.

Denote the entries of an eigenvector ${\bf u}$ of K satisfying the eigenequation $K{\bf u}=\lambda {\bf u}$ as

$$\mathbf{u} = \begin{pmatrix} u_1^a & u_1^b & u_2^a & u_2^b & \cdots & u_N^a & u_N^b \end{pmatrix}^T.$$
 (14)

Since we are discussing boundary zero modes, the $\lambda \to 0$ limit is taken at first. In terms of the Toeplitz K-matrices in the form of Eq. (2), the entries of a trial solution ${\bf u}$ to boundary zero mode are required to satisfy the recurrence relation

$$B\begin{pmatrix} u_{j-1}^a \\ u_{j-1}^b \end{pmatrix} + A\begin{pmatrix} u_j^a \\ u_j^b \end{pmatrix} + B^T \begin{pmatrix} u_{j+1}^a \\ u_{j+1}^b \end{pmatrix} = 0$$
 (15)

for $j=2,\ldots,N-1$. Moreover, **u** is required to satisfy the "boundary conditions"

$$A \begin{pmatrix} u_1^a \\ u_1^b \end{pmatrix} + B^T \begin{pmatrix} u_2^a \\ u_2^b \end{pmatrix} = 0, \tag{16a}$$

$$B\begin{pmatrix} u_{N-1}^a \\ u_{N-1}^b \end{pmatrix} + A\begin{pmatrix} u_N^a \\ u_N^b \end{pmatrix} = 0.$$
 (16b)

Eq. (16a) and Eq. (16b) are also dubbed "lower boundary condition" and "upper boundary condition", respectively. To solve the recurrence relation Eq. (15) as well as the boundary conditions Eq. (16a) and Eq. (16b), we take the following ansatz

$$\mathbf{u} = \sum_{j} c_{j} \mathbf{w}^{j},\tag{17}$$

where $\{c_j\}$ are coefficients yet to be determined and $\{\mathbf{w}^j\}$ are dubbed as "boundary basis". We assume that the a boundary base \mathbf{w}^j has the form

$$\mathbf{w}^{j} = (\beta_{j} w^{j,a} \ \beta_{j} w^{j,b} \ \beta_{j}^{2} w^{j,a} \ \beta_{j}^{2} w^{j,b} \ \cdots \ \beta_{j}^{N} w^{j,a} \ \beta_{j}^{N} w^{j,b})^{T}.$$
(18)

The recurrence relation Eq. (15) gives the equation for $\begin{pmatrix} w^{j,a} & w^{j,b} \end{pmatrix}^T$,

$$B\begin{pmatrix} w^{j,a} \\ w^{j,b} \end{pmatrix} + \beta_j A \begin{pmatrix} w^{j,a} \\ w^{j,b} \end{pmatrix} + \beta_j^2 B^T \begin{pmatrix} w^{j,a} \\ w^{j,b} \end{pmatrix} = 0.$$
 (19)

Nontrivial solution to $(w^{j,a} \ w^{j,b})^T$ renders the equation for β_j

$$\det(B + A\beta_j + B^T \beta_j^2) = 0. (20)$$

Therefore, $\{\beta_j\}$ are the solutions to the equation

$$\alpha_1 + \alpha_2 \beta + \alpha_3 \beta^2 + \alpha_2 \beta^3 + \alpha_1 \beta^4 = 0,$$
 (21)

$$\begin{cases}
\alpha_1 = l_1 l_4 - l_2 l_3, \\
\alpha_2 = -(m(l_2 + l_3) - n l_4), \\
\alpha_3 = -(l_2^2 + l_3^2 - 2 l_1 l_4 + m^2).
\end{cases} (22)$$

 β_j together with the normalization condition $(\mathbf{w}^j)^\dagger \mathbf{w}^j = 1$ settles down the entries of \mathbf{w}^j . Furthermore, we require that \mathbf{u} localizes at one z-boundary, i.e., all the $\{\beta_j\}$ in one trial solution \mathbf{u} satisfies either $|\beta_j| > 1$ or $|\beta_j| < 1$. If a trial solution \mathbf{u} is a linear combination of boundary bases $\{\mathbf{w}^j\}$ with $|\beta_j| < 1$, the boundary condition Eq. (16b) is automatically satisfied in the thermodynamical limit $2N \to \infty$. Hence our task is to verify whether a linear combination of boundary bases (given

by Eq. (17)) exists, matching the lower boundary condition Eq. (16a). Likewise, for boundary bases $\{\mathbf{w}^j\}$ with $|\beta_j|>1$, our task is to verify whether a linear combination of boundary bases matching the upper boundary condition Eq. (16b) exists. If \mathbf{u} satisfies the lower boundary condition Eq. (16a), it is referred to as lower boundary zero mode. If \mathbf{u} satisfies the upper boundary condition Eq. (16b), it is referred to as upper boundary zero mode. Following this framework, we can systematically determine whether a given K-matrix possesses boundary zero modes.

In the preceding discussion, we made the assumption that the K-matrix is infinite-dimensional. However, in the study of *Toeplitz braiding*, we calculate the inverse of a K-matrix before taking the thermodynamic limit $2N \to \infty$. Therefore, it becomes essential to incorporate the discussion on the boundary zero modes and the corresponding exponentially-suppressed eigenvalues of a *finite-size* K-matrix. If an infinite-dimensional K-matrix possesses two boundary zero modes, \mathbf{u}^1 and \mathbf{u}^2 , satisfying distinct boundary conditions Eq. (16a) and Eq. (16b), respectively, the actual boundary zero modes for a *finite-size* K-matrix are linear combinations of \mathbf{u}^1 and \mathbf{u}^2 , which can be obtained by diagonalizing the matrix

$$\begin{pmatrix} (\mathbf{u}^1)^{\dagger} K \mathbf{u}^1 & (\mathbf{u}^1)^{\dagger} K \mathbf{u}^2 \\ (\mathbf{u}^2)^{\dagger} K \mathbf{u}^1 & (\mathbf{u}^2)^{\dagger} K \mathbf{u}^2 \end{pmatrix}. \tag{23}$$

For instance, for a finite-size K_1 -type matrix, the boundary zero modes \mathbf{u}^1 and \mathbf{u}^2 meeting distinct boundary conditions are presented in Eq. (8a) and Eq. (8b). The actual boundary zero modes \mathbf{v}_1 , \mathbf{v}_2 (Eq. (7a) and Eq. (7b)) and the corresponding exponentially suppressed eigenvalues of K_1^{2N} , are obtained by diagonalizing

$$\begin{pmatrix} (\mathbf{u}^{1})^{\dagger} K_{1}^{2N} \mathbf{u}^{1} & (\mathbf{u}^{1})^{\dagger} K_{1}^{2N} \mathbf{u}^{2} \\ (\mathbf{u}^{2})^{\dagger} K_{1}^{2N} \mathbf{u}^{1} & (\mathbf{u}^{2})^{\dagger} K_{1}^{2N} \mathbf{u}^{2} \end{pmatrix} \\
= \frac{1 - \left(\frac{m}{l}\right)^{2}}{1 - \left(\frac{m}{l}\right)^{2N}} \begin{pmatrix} 0 & m\left(-\frac{m}{l}\right)^{N-1} \\ m\left(-\frac{m}{l}\right)^{N-1} & 0 \end{pmatrix}. \tag{24}$$

Having \mathbf{v}_1 , \mathbf{v}_2 and the exponentially suppressed eigenvalues λ_1 , λ_2 , we are able to construct the matrix M_1^{2N} (Eq. (12)), which captures the braiding statistics between topological excitations residing at distinct z-boundaries.

If an infinite-dimensional K-matrix possesses only one boundary zero mode ${\bf u}$ meeting either Eq. (16a) or Eq. (16b), it is in fact not an actual boundary zero mode for a *finite-size* K-matrix due to the violation to the other boundary condition. The violation will provide a minor correction to the entries of ${\bf u}$, contributing a small but nonzero eigenvalue λ , which enables the calculation of the inverse of K. In Sec. IV, we will demonstrate that $M=\frac{1}{\lambda}{\bf u}{\bf u}^{\dagger}$ also captures the braiding statistics of topological excitations residing at distinct z-boundaries, in analogy to the cases of two boundary zero modes.

In the subsequent subsections, we provide a detailed discussion on sorting the Type-I and Type-II Toeplitz K-matrices. For a K-matrix as shown in Eq. (2), we follow a two-step procedure. First, we solve for all the boundary bases, then we verify whether a linear superposition of these boundary

bases exists, as expressed in Eq. (17), satisfying either the upper boundary condition Eq. (16a) or lower boundary condition Eq. (16b). Therefore, for a given (twisted) topological order described by $A = \begin{pmatrix} n & m \\ m & 0 \end{pmatrix}$, we can identify the specific Chern-Simons coupling associated with the block B in the K-matrix that enables Toeplitz braiding. We organize our analysis based on whether the determinant of matrix B is equal to zero or not. det B plays a crucial role in determining the order of Eq. (21), which affects the # of boundary bases.

B. Discussion on block B

If det $B=\alpha_1=0$, Eq. (21) has a solution $\beta_0=0$, which is discarded. The other two solutions β_1 and β_2 , are determined by the equation

$$\alpha_2 + \alpha_3 \beta_{1,2} + \alpha_2 \beta_{1,2}^2 = 0, \tag{25}$$

from which we know that $\beta_1\beta_2=1$. For the sake of convenience, we set $|\beta_1|<1$, $|\beta_2|>1$. The bulk recurrence relation Eq. (19) together with normalization condition gives the solution to $(w^{j,a}\ w^{j,b})^T$, j=1,2. If $\mathbf{u}^1=\mathbf{w}^1$ is a legitimate boundary zero mode, it satisfies the boundary condition Eq. (16a). Detailed calculation in Appendix A 1 shows that there exists one boundary zero mode satisfying the lower boundary condition Eq. (16a) if

$$\begin{cases}
 m \neq 0, \quad l_2 \neq l_3, \\
 l_1 l_4 = l_2 l_3, \\
 2 l_3 m = l_4 n, \\
 |m| < |l_3 - l_2|,
\end{cases}
\text{ or }
\begin{cases}
 m \neq 0, \quad l_3 \neq 0, \\
 l_2 = l_4 = 0, \\
 |m| < |l_3|.
\end{cases}$$
(26)

Likewise, there exists boundary zero mode $\mathbf{u}^2 = \mathbf{w}^2$ satisfying upper boundary condition Eq. (16b) if

$$\begin{cases}
 m \neq 0, \quad l_2 \neq l_3, \\
 l_1 l_4 = l_2 l_3, \\
 2 l_2 m = l_4 n, \\
 |m| < |l_3 - l_2|.
\end{cases}
\text{ or }
\begin{cases}
 m \neq 0, \quad l_2 \neq 0, \\
 l_3 = l_4 = 0, \\
 |m| < |l_2|.
\end{cases}$$
(27)

Combining the condition (26) and (27), we conclude that if

$$\begin{cases}
 m \neq 0, & l_2 \neq 0, \\
 l_1 = l_3 = l_4 = 0, & \text{or} \\
 |m| < |l_2|, &
\end{cases}$$

$$\begin{cases}
 m \neq 0, & l_3 \neq 0, \\
 l_1 = l_2 = l_4 = 0, \\
 |m| < |l_3|,
\end{cases}$$
(28)

the K-matrix exhibits two boundary zero modes. Otherwise, if $\det B=0$, and the elements of Eq. (2) satisfies only one of the two conditions (26) and (27), the K-matrix possesses only 1 boundary zero mode.

If $\alpha_1 = \det B \neq 0$, Eq. (21) is a fourth-degree equation. It has 4 solutions β_1 , β_2 , β_3 , β_4 , satisfying $\beta_1\beta_2\beta_3\beta_4 = 1$, while solutions β_1 , β_2 satisfies $|\beta_1| < 1$, $|\beta_2| < 1$ while the other two satisfies $|\beta_3| > 1$, $|\beta_4| > 1.5$ Therefore, a legitimate boundary zero mode satisfying boundary condition

⁵ The definitions of β_1 , β_2 , β_3 , β_4 are different from those presented in Appendix A 2.

Eq. (16a) is a linear combination of \mathbf{w}^1 and \mathbf{w}^2 given by Eq. (18). Likewise, a legitimate boundary zero mode satisfying boundary condition (16b) is a linear combination of \mathbf{w}^3 and \mathbf{w}^4 given by Eq. (18). In general, analyzing the fourth-order equation Eq. (21) is very challenging. It often requires a case-by-case study to determine whether a given K-matrix possesses boundary zero modes. However, if $l_4 = 0$, Eq. (21) can be factorized into the product of two quadratic polynomials.

$$(l_2 + m\beta + l_3\beta^2)(l_3 + m\beta + l_2\beta^2) = 0,$$
 (29)

which enables a thorough discussion. Detailed analysis are shown in Appendix A 2. We discover that if

$$\begin{cases}
l_4 = 0, \\
|m| < |l_2 + l_3|, \\
n(l_2 + l_3) \neq 2l_1 m, \\
l_2 \neq l_3, \quad l_2 l_3 \neq 0,
\end{cases}$$
(30)

the K-matrix possesses one boundary zero mode. More specifically, for the case $|l_2| < |l_3|$, the boundary zero mode satisfies the lower boundary condition Eq. (A8); for the case $|l_2| > |l_3|$, the boundary zero mode satisfies the lower boundary condition Eq. (A9). If

$$\begin{cases}
l_4 = 0, \\
|m| < |l_2 + l_3|, \\
n(l_2 + l_3) = 2l_1 m, \\
l_2 \neq l_3, \quad l_2 l_3 \neq 0,
\end{cases}$$
(31)

the K-matrix possesses two boundary zero modes.

C. Condition for Type-I and Type-II iCS field theories

Combining (28) and (31), we conclude that if the elements of the K-matrix satisfy

$$\begin{cases}
|m| < |l_2 + l_3| \\
l_4 = 0 \\
n(l_2 + l_3) = 2l_1 m
\end{cases}$$
(32)

the K-matrix exhibits two boundary zero modes, and the corresponding iCS field theory is a Type-I theory. Furthermore, combining the condition (26), (27) and (30), we conclude that if the elements of K-matrix satisfy

$$\begin{cases} |m| < |l_2 + l_3| \\ l_4 = 0 \\ n(l_2 + l_3) \neq 2l_1 m \end{cases} \text{ or } \begin{cases} |m| < |l_2 - l_3| \\ l_4 \neq 0 \\ \det B = l_1 l_4 - l_2 l_3 = 0 \\ (2l_2 m - l_4 n)(2l_3 m - l_4 n) = 0 \end{cases} ,$$

$$(33)$$

the K-matrix possesses only 1 boundary zero zero mode, and the corresponding iCS field theory is a Type-II iCS field theory. The aforementioned K_1^{2N} matrix, in its mathematical form, is equivalent to the single-particle Hamiltonian of a typical 1d topological insulator i.e., the SSH model. Since K_1^{2N}

has two boundary zero modes, it belongs to Type-I iCS field theory. Generally speaking, Type-I K-matrix has been widely discussed in the study of TI and TSC. The presence of boundary zero mode, as is well-known, can be indicated by topological invariants. However, the Toeplitz matrices with only one boundary zero mode, i.e., the Type-II Toeplitz K-matrices, are rarely studied in the context of TI and TSC. Although we draw comparisons between the K-matrices of iCS field theories and the Hamiltonians of TI and TSC, it is important to note that the occurrence of Toeplitz braiding does not require any symmetry protection.

In order to demonstrate the nonlocal braiding statistics (Toeplitz braiding) along the z-direction in Type-I and Type-II iCS field theories, we present a numerical computation in the upcoming section.

IV. NUMERICAL COMPUTATION ON TOEPLITZ BRAIDING

In this section, we conduct a numerical computation that illustrates the connection between the appearance of nonlocal braiding statistics in z-direction and the existence of boundary zero modes of K-matrix. For comparative analysis, we focus on iCS field theories that arise from stacking \mathbb{Z}_2 twisted topological orders. The block A in the K-matrix, given by (2), is $\begin{pmatrix} 2 & 2 \\ 2 & 0 \end{pmatrix}$ which describes the double-semion topological order.

A. Numerical computation on Toeplitz braiding via Type-I and Type-II iCS field theories

To demonstrate the correspondence between boundary zero modes and Toeplitz braiding in Type-I and Type-II iCS field theories, we consider three iCS field theories as illustrative examples without loss of generality. The K-matrix (Eq. (2)) are denoted as K_2^{2N} , K_3^{2N} and K_4^{2N} , where 2N is the system size as well as the size of the K-matrix. Block A and block B in K_2^{2N} , K_3^{2N} and K_4^{2N} matrices are denoted as A_j and B_j (j=2,3,4), where

$$A_2 = A_3 = A_4 = \begin{pmatrix} 2 & 2 \\ 2 & 0 \end{pmatrix} \tag{34}$$

and B_j (j = 2, 3, 4) reads

$$B_2 = \begin{pmatrix} 2 & 1 \\ 3 & 0 \end{pmatrix}, \quad B_3 = \begin{pmatrix} 2 & 4 \\ 1 & 2 \end{pmatrix}, \quad B_4 = \begin{pmatrix} 2 & 1 \\ 4 & 2 \end{pmatrix}. \quad (35)$$

The elements of K_2^{2N} satisfy the condition (31) in Sec. III, implying that K_2^{2N} has two boundary zero modes. Therefore, the corresponding iCS field theory is a Type-I iCS field theory. The elements of K_3^{2N} satisfy the condition (26), whereas K_4^{2N} satisfy the condition (27). Therefore, K_3^{2N} possess one lower boundary zero mode while K_4^{2N} exhibit one upper boundary zero modes. They belong to Type-II iCS field theories. To demonstrate the nonlocal braiding statistics encoded in these iCS field theories, i.e., the *Toeplitz braiding*, we

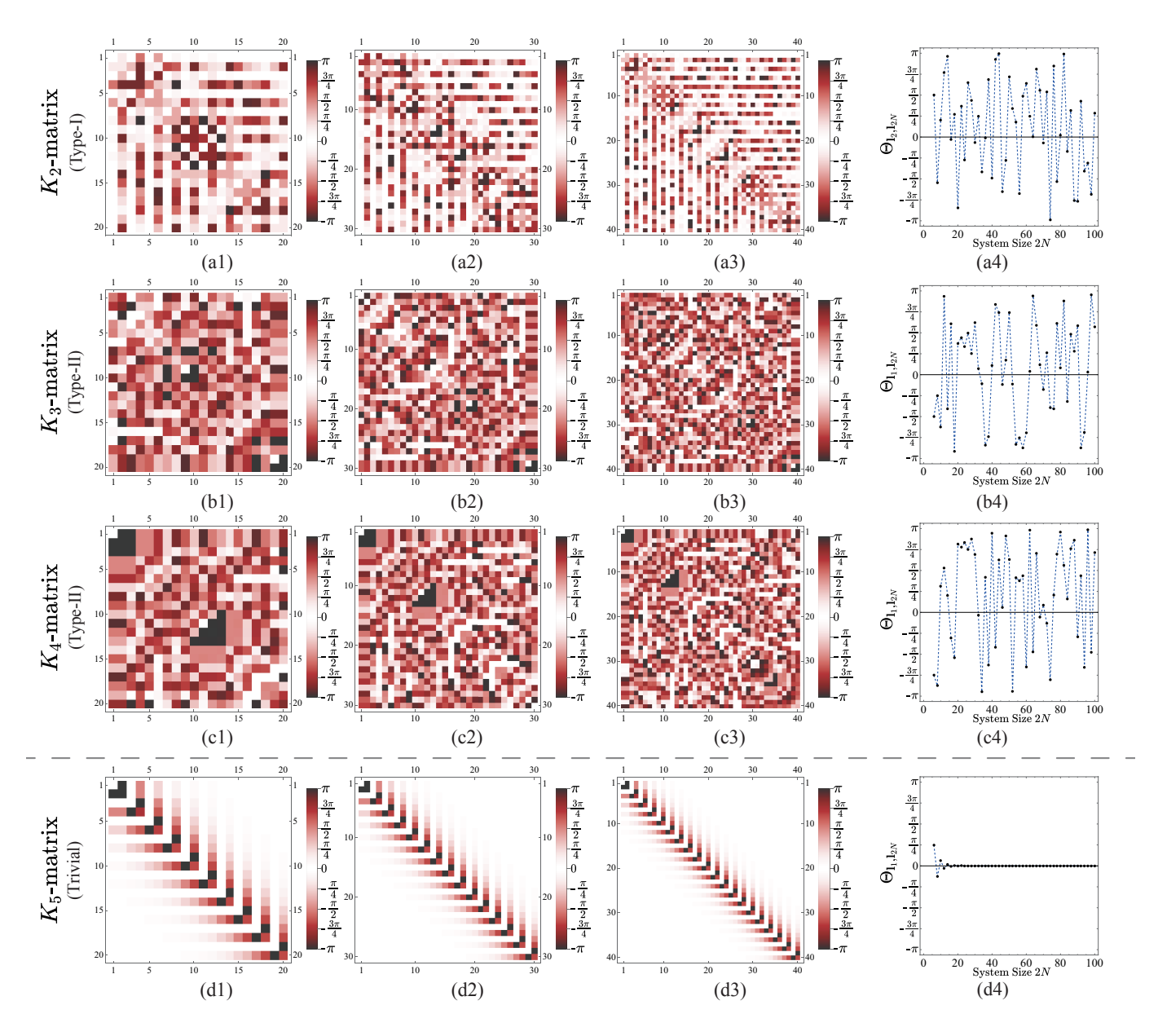


FIG. 5. (a1-a3), (b1-b3) and (c1-c3) are the matrix plots of mutual braiding phase angle $\Theta_{1_I,1_J}=2\pi I_I^T(K_{2,3,4}^{2N})^{-1}1_J$, where we take the system size 2N=20,30,40 and the mutual braiding phase angle is limited to $[-\pi,\pi)$. (a4), (b4) and (c4) show that the mutual braiding phase angle between topological excitations residing at distinct z-boundaries exhibit oscillation as the system size 2N increases, where we choose $\Theta_{1_2,1_{2N}}$ or $\Theta_{1_1,1_{2N}}$ as a representative. (d4) demonstrates the braiding phase angle between topological excitations residing at distinct z-boundaries decreases drastically as the system size 2N increases in K_5 -matrix (trivial) iCS field theory, where we select $\Theta_{1_1,1_{2N}}$ as a representative.

numerically compute the braiding statistics encoded in finite-size K-matrices of different dimensions, from which how the braiding statistics scale with system size is known. The mutual braiding phase angle $\Theta_{1_I,1_J}$ is presented in Fig. 5, where $\Theta_{1_I,1_J}$ (Eq. (16a)) is the mutual braiding phase angle between topological excitations carrying unit gauge charge (Eq. (6)). Fig. 5(a1-a3), Fig. 5(b1-b3) and Fig. 5(c1-c3) are the matrix plots of mutual braiding phase angle $\Theta_{1_I,1_J}$ of K_2 -matrix, K_3 -matrix and K_4 -matrix iCS field theories, respectively, where we set the size of the K-matrix to be 20, 30 and 40. Numerical results show the robust presence of non-zero elements in

the upper-right and lower-left positions of the matrices upon the system size is enlarged, which is vital to Toeplitz braiding. Fig. 5(a4) shows that how the mutual braiding phase angle $\Theta_{\mathbf{l}_2,\mathbf{l}_{2N}}$ changes with respect to the system size 2N, while Fig. 5(b4) and Fig. 5(c4) show how the mutual braiding phase angle $\Theta_{\mathbf{l}_1,\mathbf{l}_{2N}}$ changes with respect to the system size 2N. From the numerical results, we clearly find that the phase angle oscillates as the system size 2N increases, indicative of the existence of Toeplitz braiding.

To more clearly understand the nontriviality of Toeplitz braiding, it is beneficial to make a sharp comparison by

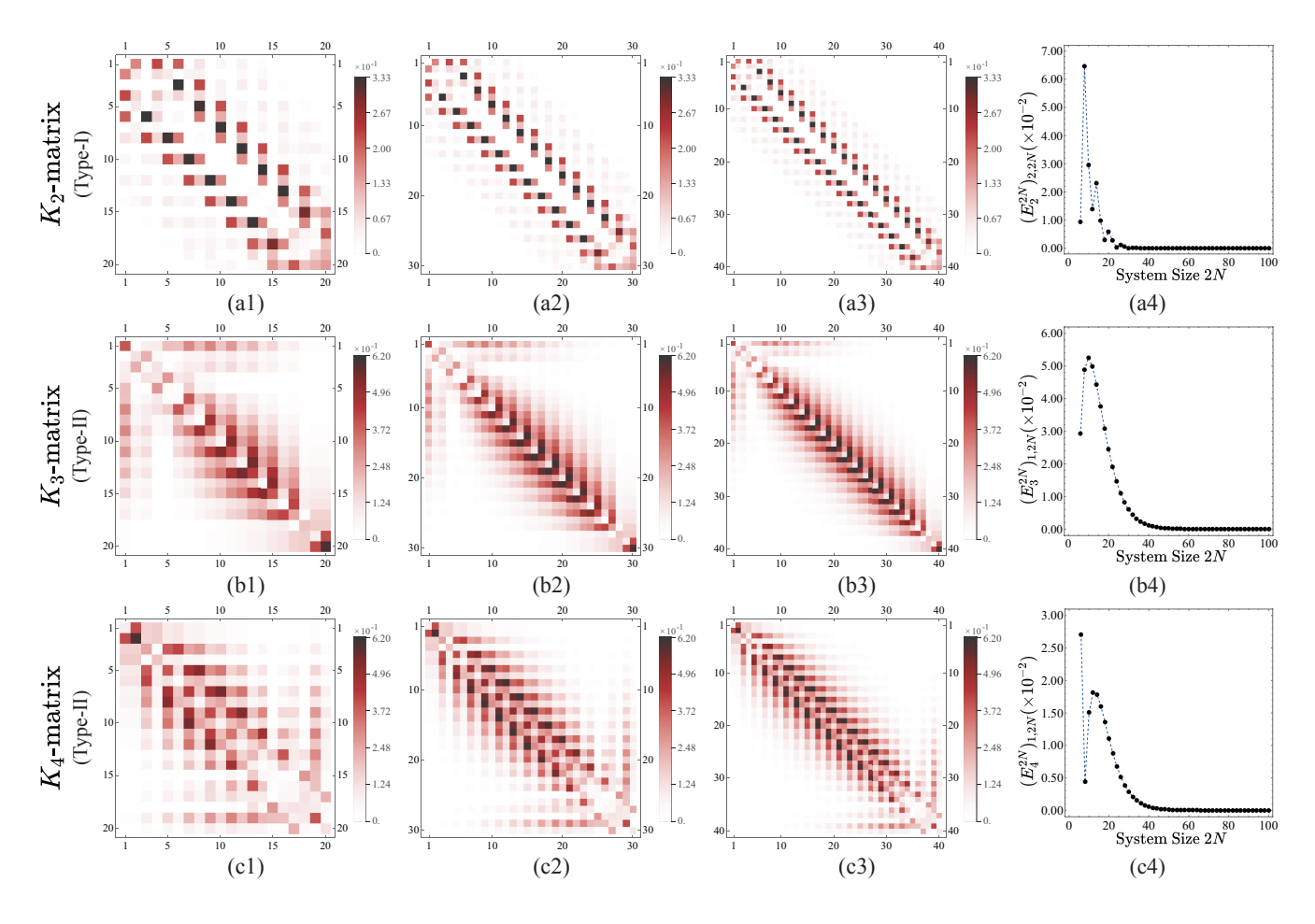


FIG. 6. (a1-a3), (b1-b3) and (c1-c3) are the matrix plots of E_2^{2N} , E_3^{2N} and E_4^{2N} , where we select 3 representative system size 2N=20,30,40 for each type of iCS field theory. The presence of blank space in the upper-right and lower-left indicates that the matrices M_2^{2N} , M_3^{2N} and M_4^{2N} can effectively describe the braiding statistics between topological excitations residing at distinct z-boundaries. (a4), (b4) and (c4) shows that the upper-right and lower-left elements of E_2^{2N} , E_3^{2N} and E_4^{2N} decrease drastically as the system size E_4^{2N} increases, where we choose E_2^{2N} , E_3^{2N} and E_4^{2N} are representatives.

demonstrating what we expect for the K-matrix that doesn't support Toeplitz braiding. For this purpose, we consider a new K-matrix denoted as K_5^{2N} , composed of the following A and B blocks

$$A_5 = \begin{pmatrix} 2 & 2 \\ 2 & 0 \end{pmatrix}, \quad B_5 = \begin{pmatrix} 0 & 1 \\ 0 & 0 \end{pmatrix}. \tag{36}$$

Fig. 5(d1-d3) are the matrix plots of the mutual braiding phase angle $\Theta_{\mathbf{l}_I,\mathbf{l}_J}$ encoded in K_5^{2N} , where we also set the matrix size 2N=20,30,40 during the numerical computation. The mutual braiding phase angle $\Theta_{\mathbf{l}_I,\mathbf{l}_J}$ decreases with |I-J|, i.e., the distance in z between topological excitations. If two topological excitations are sufficiently far apart in z-direction, they cannot detect each other by braiding. Fig. 5(d4) shows how the mutual braiding phase angle $\Theta_{\mathbf{l}_1,l_{2N}}$ decreases drastically as the system size 2N increases, which also demonstrates that the topological excitations residing at distinct z-boundaries cannot detect each other via braiding.

B. Numerical computation on the relation between Toeplitz braiding and boundary zero modes

In Sec. II, we have shown that the braiding statistics between topological excitations at distinct z-boundaries is captured by boundary zero modes. Following this thought, we carry on a numerical computation, demonstrating that the correspondence still holds in K_2 -, K_3 - and K_4 -matrix iCS field theories. In analogy to Eq. (12) in Sec. II, for Type-I iCS field theories with two boundary zero modes \mathbf{v}_1 and \mathbf{v}_2 , we claim that the braiding statistics between topological excitations residing at distinct z-boundaries are captured by

$$M = \frac{1}{\lambda_1} \mathbf{v}_1 \mathbf{v}_1^{\dagger} + \frac{1}{\lambda_2} \mathbf{v}_2 \mathbf{v}_2^{\dagger}, \tag{37}$$

where λ_1 and λ_2 are the corresponding exponentially suppressed eigenvalues of \mathbf{v}_1 and \mathbf{v}_2 . As is discussed in Sec. III, for Type-II iCS field theories with only one boundary zero mode \mathbf{v} , we may also introduce a matrix M constructed by the only boundary zero mode and the corresponding exponen-

tially suppressed eigenvalue λ ,

$$M = \frac{1}{\lambda} \mathbf{v} \mathbf{v}^{\dagger}. \tag{38}$$

The matrix M constructed by the boundary zero modes of K_2^{2N} , K_3^{2N} and K_4^{2N} are denoted as M_2^{2N} , M_3^{2N} and M_4^{2N} , respectively. Compared to the inverse of the K_2^{2N} , K_3^{2N} and K_4^{2N} , M_2^{2N} , M_3^{2N} and M_4^{2N} provide a good asymptotic approximation to the upper-right and lower-left elements, as depicted in Fig. 6(a1-a3), Fig. 6(b1-b3) and Fig. 6(c1-c3), where we define matrices E_j^{2N} with element $(E_j^{2N})_{IJ} = |(M_j^{2N})_{IJ} - [(K_j^{2N})^{-1}]_{IJ}| \ (j=2,3,4)$ to characterize the difference between the two matrices K_j^{-1} an M_j . To illustrate, we choose 2N=20,30,40 for each type of iCS field theories. As 2N increases, the upper-right and lower-left elements of M_j^{2N} and $(K_j^{2N})^{-1}$ (j=2,3,4) converge towards each other, as shown in Fig. 5(a4), Fig. 5(b4) and Fig. 5(c4), where we focus on the asymptotic behavior of $(E_2^{2N})_{2,2N}$, $(E_3^{2N})_{1,2N}$ and $(E_4^{2N})_{1,2N}$ as representatives. This observation suggests that we can extract information about the braiding statistics of excitations residing at distinct z-boundaries by analyzing the zero modes and their "close-to-zero" eigenvalues.

V. CONCLUSIONS

In this paper, we constructed a type of 3D topological fracton topological orders whose surface states support a nontrivial form of braiding statistics, termed *Toeplitz braiding*. This boundary phenomenon arises due to the block-tridiagonal Toeplitz structure of the *K*-matrix in the infinite-component Chern-Simons theory. This phenomenon represents a significant departure from conventional braiding statistics observed in 2D topological orders. Here, we further summarize the paper in details. First, in the field of free-fermion topological insulators, boundary zero modes of Toeplitz matrices play a vital role. In this paper, we substantially extend the topological physics of boundary zero modes of Toeplitz matrices to the present strongly correlated systems. Second, our research categorizes nontrivial *K*-matrices into two distinct types based

on their boundary zero modes. This classification provides a deeper understanding of the underlying mathematical structures and their physical implications in 3D fracton topological orders. Third, we conduct extensive numerical simulations and finite-size scaling analyses to confirm the theoretical predictions. These simulations demonstrate the robustness of Toeplitz braiding.

There are several future directions. First of all, it will be interesting to construct the lattice model realization of iCS field theories that supports boundary Toeplitz braiding, which may pave the way for further numerical or experimental study on Toeplitz braiding. From the perspective of fractional quantum Hall states or spin liquid, the stacking process described in Sec. II A can be realized by condensing topological excitations followed by adding interlayer interaction of condensation currents or spin-spin interaction [12, 15, 43, 44], which may be also useful here. Detailed construction that explicitly enables Toeplitz braiding will be left to future discussion. Furthermore, following the construction of topologicallyordered non-liquid states in this paper, the construction of higher-dimensional topologically-ordered non-liquid states is directly allowed. For instance, by stacking (3+1)D topological orders [45–48], we can obtain a (4+1)D topologically-ordered non-liquid state. Similarly, stacking (2+1)D topological orders in two independent spatial dimensions can also yield (4+1)D topologically-ordered non-liquid states. The study of these theories and the duality between them is left for future research. We can also compute entanglement entropy via partitioning the system into two subsystems along z directions and study whether and how the presence of Toeplitz braiding leaves its fingerprint in the scaling behavior of entanglement entropy.

ACKNOWLEDGMENTS

This work was supported by National Natural Science Foundation of China (NSFC) Grant No. 12074438 and Guangdong Provincial Key Laboratory of Magnetoelectric Physics and Devices under Grant No. 2022B1212010008.

Appendix A: Detailed Derivation on Sorting Boundary Zero Modes of Toeplitz K-matrices

The Appendix provides further discussions on the technical details of sorting boundary zero modes of the K-matrix in Sec. III of the main text. To make reading easier, we list the key equations from the main text below: A trial solution \mathbf{u} of boundary zero mode is a linear combination of boundary bases $\{\mathbf{w}^j\}$:

$$\mathbf{u} = \sum_{j} c_{j} \mathbf{w}^{j}. \tag{A1}$$

A boundary base \mathbf{w}^j has the form

$$\mathbf{w}^{j} = (\beta_{j} w^{j,a} \ \beta_{j} w^{j,b} \ \beta_{j}^{2} w^{j,a} \ \beta_{j}^{2} w^{j,b} \ \cdots \ \beta_{j}^{N} w^{j,a} \ \beta_{j}^{N} w^{j,b})^{T}, \tag{A2}$$

which is required to satisfy the bulk recurrence relation

$$B\begin{pmatrix} w^{j,a} \\ w^{j,b} \end{pmatrix} + \beta_j A \begin{pmatrix} w^{j,a} \\ w^{j,b} \end{pmatrix} + \beta_j^2 B^T \begin{pmatrix} w^{j,a} \\ w^{j,b} \end{pmatrix} = 0.$$
 (A3)

Nontrivial solution to $(w^{j,a} \ w^{j,b})^T$ renders the equation for β_j

$$\det(B + A\beta_j + B^T \beta_j^2) = 0. (A4)$$

Therefore, $\{\beta_j\}$ are the solutions to the equation

$$\alpha_1 + \alpha_2 \beta + \alpha_3 \beta^2 + \alpha_2 \beta^3 + \alpha_1 \beta^4 = 0, (A5)$$

$$\begin{cases}
\alpha_1 = l_1 l_4 - l_2 l_3, \\
\alpha_2 = -(m(l_2 + l_3) - n l_4), \\
\alpha_3 = -(l_2^2 + l_3^2 - 2 l_1 l_4 + m^2).
\end{cases}$$
(A6)

If det $B = \alpha_1 = 0$, Eq. (A5) has a solution $\beta_0 = 0$, which is discarded. The other two solutions β_1 and β_2 , are determined by the equation

$$\alpha_2 + \alpha_3 \beta_{1,2} + \alpha_2 \beta_{1,2}^2 = 0, (A7)$$

from which we know that $\beta_1\beta_2=1$. ${\bf u}$ is required to localize at one z-boundary, i.e., all the $\{\beta_j\}$ in one trial solution ${\bf u}$ satisfies either $|\beta_j|>1$ or $|\beta_j|<1$. If a trial solution ${\bf u}$ is a linear combination of boundary bases $\{{\bf w}^j\}$ with $|\beta_j|<1$, it is required to match the boundary condition

$$A \begin{pmatrix} u_1^a \\ u_1^b \end{pmatrix} + B^T \begin{pmatrix} u_2^a \\ u_2^b \end{pmatrix} = 0. \tag{A8}$$

If a trial solution ${\bf u}$ is a linear combination of boundary bases $\{{\bf w}^j\}$ with $|\beta_j|>1$, it is required to match the boundary condition

$$B\begin{pmatrix} u_{N-1}^a \\ u_{N-1}^b \end{pmatrix} + A\begin{pmatrix} u_N^a \\ u_N^b \end{pmatrix} = 0.$$
 (A9)

As is discussed in the main text, we classify our discussion based on the order of Eq. (A5), which affects the # of boundary bases. A detailed discussion on $\det B = 0$ cases are presented in Sec. A 1, while a detailed discussion on $\det B \neq 0$ cases are presented in Sec. A 2.

1. $\det B = 0$

Discussion on \mathbf{w}^1 satisfying the boundary condition Eq. (A8) If $l_4 \neq 0$, for the boundary base \mathbf{w}^1 with entries

$$\mathbf{w}^{1} = \begin{pmatrix} \beta_{1} w^{1,a} & \beta_{1} w^{1,b} & \beta_{1}^{2} w^{1,a} & \beta_{1}^{2} w^{1,b} & \cdots & \beta_{1}^{N} w^{1,a} & \beta_{1}^{N} w^{1,b} \end{pmatrix}^{T}, \tag{A10}$$

the bulk recurrence relation Eq. (A3) is solved by

$$w^{1,a} = l_4(1+\beta_1^2)c_1, \quad w^{1,b} = -(l_3 + m\beta_1 + l_2\beta_1^2)c_1,$$

where $c_1 \neq 0$ is a normalization constant. Since $0 < |\beta_1| < 1$, \mathbf{w}^1 is required to satisfy the boundary condition Eq. (A8), which renders

$$\beta_1 \left(\beta_1 \left(\beta_1^2 + 1 \right) l_1 l_4 - m \left(\beta_1 (\beta_1 l_2 + m) + l_3 \right) - \beta_1 l_3 \left(\beta_1 (\beta_1 l_2 + m) + l_3 \right) + \left(\beta_1^2 + 1 \right) l_4 n \right) = 0, \tag{A11a}$$

$$\beta_1 l_4 (\beta_1 (l_2 - l_3) + m) = 0. \tag{A11b}$$

If $l_4 \neq 0$, Eq. (A11b) implies $\beta_1(l_2-l_3)+m=0$, rendering either $\left\{ \begin{array}{l} l_2=l_3\\ m=0 \end{array} \right.$ or $\beta_1=\frac{m}{l_3-l_2}$. $\left\{ \begin{array}{l} l_2=l_3\\ m=0 \end{array} \right.$ together with Eq. (A11a) enforces $|\beta_1|=1$ or $|\beta_1|=0$, which does not correspond to a boundary zero mode and should be discarded. Hence we shall continue with $\beta_1=\frac{m}{l_3-l_2}$. Since $l_4\neq 0$, we can safely set $l_1=l_2l_3/l_4$. Eq. (A11a) and Eq. (A7) render

$$\frac{\left((l_2 - l_3)^2 + m^2\right)(2l_3m - l_4n)}{(l_2 - l_3)^2} = 0.$$

Therefore, if $2l_3m - l_4n = 0$, Eq. (A10) represents a boundary state that satisfies the boundary condition Eq. (A8). Taking the aforementioned conditions into account, if

$$\begin{cases} m \neq 0, \quad l_4 \neq 0, \quad l_2 \neq l_3, \\ l_1 l_4 = l_2 l_3, \quad 2l_3 m = l_4 n, \\ |m| < |l_3 - l_2|, \end{cases}$$

then there exists one boundary zero mode $\mathbf{u}^1 = \mathbf{w}^1$ given by Eq. (A10), where

$$w^{1,a} = \frac{l_4}{\beta_1 \sqrt{l_3^2 + l_4^2}} \sqrt{\frac{1 - \beta_1^2}{1 - \beta_1^{2N}}}, \quad w^{1,b} = -\frac{l_3}{\beta_1 \sqrt{l_3^2 + l_4^2}} \sqrt{\frac{1 - \beta_1^2}{1 - \beta_1^{2N}}}, \quad \beta_1 = \frac{m}{l_3 - l_2}.$$

The above discussion ignored $l_4 = 0$. If $l_4 = 0$, $\det B = 0$ necessitates $l_2 l_3 = 0$. If $l_2 = l_3 = l_4 = 0$, i.e.

$$A = \begin{pmatrix} n & m \\ m & 0 \end{pmatrix}, \quad B = \begin{pmatrix} l_1 & 0 \\ 0 & 0 \end{pmatrix},$$

the bulk recurrence relation Eq. (A3) and the boundary condition Eq. (A8) render

$$\begin{pmatrix} l_1 + n\beta_1 + l_1\beta_1^2 & m\beta_1 \\ m\beta_1 & 0 \end{pmatrix} \begin{pmatrix} w^{1,a} \\ w^{1,b} \end{pmatrix} = 0, \quad \begin{pmatrix} \beta_1(n + l_1\beta_1) & m\beta_1 \\ m\beta_1 & 0 \end{pmatrix} \begin{pmatrix} w^{1,a} \\ w^{1,b} \end{pmatrix} = 0.$$
 (A12)

Nontrivial solution to Eq. (A12) enforces m=0, resulting in a zero determinant for the K-matrix. Therefore, $l_2=l_3=l_4=0$ is excluded from consideration. If $l_2=0$, $l_3\neq 0$, i.e.

$$A = \begin{pmatrix} n & m \\ m & 0 \end{pmatrix}, \quad B = \begin{pmatrix} l_1 & 0 \\ l_3 & 0 \end{pmatrix},$$

for \mathbf{w}^1 , the bulk recurrence relation Eq. (A3) is solved by

$$w^{1,a} = 0, \quad w^{1,b} = c_1, \quad \beta_1 = -\frac{m}{l_3}.$$
 (A13)

where $c_1 \neq 0$ is the normalization constant. Since $0 < |\beta_1| < 1$, \mathbf{w}^1 is required to satisfy the boundary condition Eq. (A8), which gives

$$\begin{pmatrix} \beta_1^2 l_1 + \beta_1 n & \beta_1^2 l_3 + \beta_1 m \\ \beta_1 m & 0 \end{pmatrix} \begin{pmatrix} w^{1,a} \\ w^{1,b} \end{pmatrix} = 0.$$
 (A14)

If \mathbf{w}^1 is solved by Eq. (A13), Eq. (A14) naturally holds. Therefore, if

$$\begin{cases} m \neq 0, & l_3 \neq 0, \\ l_4 = l_2 = 0, \\ |m| < |l_3|, \end{cases}$$

there exists a boundary zero mode $\mathbf{u}^1 = \mathbf{w}^1$ given by Eq. (A10), satisfying boundary condition Eq. (A8), where

$$w^{1,a} = 0$$
, $w^{1,b} = \frac{1}{\beta_1} \sqrt{\frac{1 - \beta_1^{2N}}{1 - \beta_1^2}}$, $\beta_1 = -\frac{m}{l_3}$.

If $l_3 = 0$, $l_2 \neq 0$, i.e.

$$A = \begin{pmatrix} n & m \\ m & 0 \end{pmatrix}, \quad B = \begin{pmatrix} l_1 & l_2 \\ 0 & 0 \end{pmatrix},$$

the bulk recurrence relation Eq. (A3) is solved by

$$\begin{cases} w^{1,a} = 0 \\ w^{1,b} = c_1 \\ \beta_1 = -\frac{l_2}{m} \end{cases} \text{ or } \begin{cases} w^{1,a} = -(l_2 + m\beta_1)c_1 \\ w^{1,b} = (l_1 + n\beta_1 + l_1\beta_1^2)c_1 \\ \beta_1 = -\frac{m}{l_2} \end{cases},$$

where $c_1 \neq 0$ is a normalization constant. In this condition, only if $n = l_1 = l_3 = l_4 = 0$, $|m| < |l_2|$, i.e.

$$A = \begin{pmatrix} 0 & m \\ m & 0 \end{pmatrix}, \quad B = \begin{pmatrix} 0 & l_2 \\ 0 & 0 \end{pmatrix}, \tag{A15}$$

there is a boundary zero mode $\mathbf{u}^1 = \mathbf{w}^1$ given by Eq. (A10), satisfying the boundary condition Eq. (A8), where

$$w^{1,a} = \frac{1}{\beta_1} \sqrt{\frac{1 - \beta_1^{2N}}{1 - \beta_1^2}}, \quad w^{1,b} = 0, \quad \beta_1 = -\frac{m}{l_2}.$$

Discussion on \mathbf{w}^2 satisfying the boundary condition Eq. (A9) Likewise, if $l_4 \neq 0$, for the boundary base \mathbf{w}^2 with entries

$$\mathbf{w}^2 = \begin{pmatrix} \beta_2 w^{2,a} & \beta_2 w^{2,b} & \beta_2^2 w^{2,a} & \beta_2^2 w^{2,b} & \cdots & \beta_2^N w^{2,a} & \beta_2^N w^{2,b} \end{pmatrix}^T, \tag{A16}$$

the bulk recurrence relation Eq. (A3) is solved by

$$w^{2,a} = l_4(1+\beta_2^2)c_2, \quad w^{2,b} = -(l_3+m\beta_2+l_2\beta_2^2)c_2,$$

where $c_2 \neq 0$ is a normalization constant. Since $|\beta_2| > 1$, it is required to satisfy the boundary condition Eq. (A9), rendering

$$-\left(\beta_2^2+1\right)l_4(l_1+n\beta_2)+\beta_2^2l_2^2+l_2\left(l_3+\beta_2m+\beta_2^3m\right)+\beta_2^2m(l_3+\beta_2m)=0, \tag{A17a}$$

$$l_4\beta_2^2((l_3-l_2)+m\beta_2)=0. (A17b)$$

Eq. (A17b) implies $(l_3-l_2)+m\beta_2=0$, which enforces either $\begin{cases} l_2=l_3\\ m=0 \end{cases}$ or $\beta_2=\frac{l_2-l_3}{m}$. $\begin{cases} l_2=l_3\\ m=0 \end{cases}$ enforces $|\beta_2|=0$ or $|\beta_2|=1$, which does not correspond to a boundary zero mode and should be discarded. Hence we shall continue with $\beta_2=\frac{l_2-l_3}{m}$. Since $l_4\neq 0$, we can safely set $l_1=l_2l_3/l_4$. Eq. (A17a) and Eq. (A7) render

$$\frac{\left((l_2 - l_3)^2 + m^2\right)(2l_2m - l_4n)}{(l_2 - l_3)^2} = 0.$$

Therefore, if $2l_2m - l_4n = 0$, Eq. (A16) represents a boundary zero mode that satisfies the boundary condition Eq. (A9). Taking the aforementioned conditions into account, if

$$\begin{cases} m \neq 0, \quad l_4 \neq 0, \\ l_1 l_4 = l_2 l_3, \quad 2l_2 m = l_4 n, \\ |m| < |l_3 - l_2|, \end{cases}$$

there exists one boundary zero mode $\mathbf{u}^2 = \mathbf{w}^2$ given by Eq. (A16), where

$$w^{2,a} = \frac{l_4}{\beta_2 \sqrt{l_2^2 + l_4^2}} \sqrt{\frac{1 - \beta_2^2}{1 - \beta_2^{2N}}}, \quad w^{2,b} = -\frac{l_2}{\beta_2 \sqrt{l_2^2 + l_4^2}} \sqrt{\frac{1 - \beta_2^2}{1 - \beta_2^{2N}}}, \quad \beta_2 = \frac{l_2 - l_3}{m}.$$

The above discussion ignored $l_4=0$. If $l_4=0$, $\det B=0$ enforces $l_2l_3=0$. If $l_2=l_3=l_4=0$, i.e.

$$A = \begin{pmatrix} n & m \\ m & 0 \end{pmatrix}, \quad B = \begin{pmatrix} l_1 & 0 \\ 0 & 0 \end{pmatrix},$$

the bulk recurrence relation Eq. (A3) and the boundary condition Eq. (A9) render

$$\begin{pmatrix} l_1 + n\beta_1 + l_1\beta_1^2 & m\beta_1 \\ m\beta_1 & 0 \end{pmatrix} \begin{pmatrix} w^{1,a} \\ w^{1,b} \end{pmatrix} = 0, \quad \begin{pmatrix} l_1 + n\beta_1 & m\beta_1 \\ m\beta_1 & 0 \end{pmatrix} \begin{pmatrix} w^{1,a} \\ w^{1,b} \end{pmatrix} = 0.$$
 (A18)

Nontrivial solution to Eq. (A18) enforces m=0, resulting in a zero determinant for the K-matrix. Therefore, $l_2=l_3=l_4=0$ is excluded from consideration. If $l_3=0$, $l_2\neq 0$, i.e.

$$A = \begin{pmatrix} n & m \\ m & 0 \end{pmatrix}, \quad B = \begin{pmatrix} l_1 & l_2 \\ 0 & 0 \end{pmatrix},$$

for \mathbf{w}^2 , the bulk recurrence relation Eq. (A3) is solved by

$$w^{2,a} = 0, \quad w^{2,b} = c_2, \tag{A19}$$

where $c_2 \neq 0$ is a normalization constant. Since $|\beta_2| > 1$, \mathbf{w}^2 is required to satisfy the boundary condition Eq. (A9), which gives

$$\binom{l_1 + \beta_2 n}{\beta_2 m} \binom{l_2 + \beta_2 m}{0} \binom{w^{2,a}}{w^{2,b}} = 0.$$
 (A20)

If \mathbf{w}^2 is solved by Eq. (A19), Eq. (A20) naturally holds. Therefore, if

$$\begin{cases} m \neq 0, & l_2 \neq 0, \\ l_4 = l_3 = 0, \\ |m| < |l_2|, \end{cases}$$

there exists a boundary zero mode $\mathbf{u}^2 = \mathbf{w}^2$ with

$$w^{2,a} = 0$$
, $w^{2,b} = \frac{1}{\beta_2} \sqrt{\frac{1 - \beta_2^{2N}}{1 - \beta_2^2}}$, $\beta_2 = -\frac{l_2}{m}$,

satisfying the boundary condition Eq. (A9). If $l_2 = 0$, $l_3 \neq 0$ i.e.

$$A = \begin{pmatrix} n & m \\ m & 0 \end{pmatrix}, \quad B = \begin{pmatrix} l_1 & 0 \\ l_3 & 0 \end{pmatrix},$$

the bulk recurrence relation Eq. (A3) is solved by

$$\begin{cases} w^{2,a} = -m\beta_2 c_2 \\ w^{2,b} = (l_1 + n\beta_2)c_2 \\ \beta_2 = -\frac{l_3}{m} \end{cases},$$

where $c_2 \neq 0$ is a normalization constant. In this condition, only if $n = l_1 = l_2 = l_4 = 0$, $|m| < |l_3|$, there is a boundary zero mode $\mathbf{u}^2 = \mathbf{w}^2$ given by Eq. (A16), satisfying the boundary condition Eq. (A9), where

$$w^{2,a} = \frac{1}{\beta_2} \sqrt{\frac{1 - \beta_2^{2N}}{1 - \beta_2^2}}, \quad w^{2,b} = 0, \quad \beta_2 = -\frac{l_3}{m}.$$

In summary, if

$$\begin{cases}
 m \neq 0, & n \neq 0, \\
 l_1 l_4 = l_2 l_3, \\
 2 l_3 m = l_4 n \text{ or } 2 l_2 m = l_4 n, \\
 |m| < |l_3 - l_2|,
\end{cases}$$
(A21)

the K-matrix Eq. (2) has one boundary zero mode. More specifically, if $2l_3m = l_4n$, the boundary zero mode is a lower boundary zero mode, satisfying the boundary condition Eq. (A8). If $2l_2m = l_4n$, the boundary zero mode is a upper boundary zero mode, satisfying the boundary condition Eq. (A9). If

$$\begin{cases} m \neq 0, \\ n = 0, \\ l_1 = l_3 = l_4 = 0 \text{ or } l_1 = l_2 = l_4 = 0, \\ |m| < |l_3| \text{ or } |m| < |l_2|, \end{cases}$$
(A22)

the K-matrix has two boundary zero modes.

2.
$$\det B \neq 0$$

If det $B = l_1 l_4 - l_2 l_3 \neq 0$, Eq. (A5) is a fourth-degree equation. If det $B = \alpha_1 = l_1 l_4 - l_2 l_3 \neq 0$, the solution to β is

$$\beta_{1} = \frac{-\alpha_{1}\sqrt{\frac{2\alpha_{2}\left(\sqrt{8\alpha_{1}^{2}-4\alpha_{1}\alpha_{3}+\alpha_{2}^{2}}+\alpha_{2}\right)-4\alpha_{1}\alpha_{3}}{\alpha_{1}^{2}}-8} - \sqrt{8\alpha_{1}^{2}-4\alpha_{1}\alpha_{3}+\alpha_{2}^{2}}-\alpha_{2}}{4\alpha_{1}}}{\alpha_{1}}$$

$$\beta_{2} = \frac{\alpha_{1}\sqrt{\frac{2\alpha_{2}\left(\sqrt{8\alpha_{1}^{2}-4\alpha_{1}\alpha_{3}+\alpha_{2}^{2}}+\alpha_{2}\right)-4\alpha_{1}\alpha_{3}}{\alpha_{1}^{2}}-8}-\sqrt{8\alpha_{1}^{2}-4\alpha_{1}\alpha_{3}+\alpha_{2}^{2}}-\alpha_{2}}}{4\alpha_{1}}}{\alpha_{1}},$$

$$\beta_{3} = \frac{-\alpha_{1}\sqrt{\frac{2\alpha_{2}\left(\alpha_{2}-\sqrt{8\alpha_{1}^{2}-4\alpha_{1}\alpha_{3}+\alpha_{2}^{2}}\right)-4\alpha_{1}\alpha_{3}}{\alpha_{1}^{2}}-8}+\sqrt{8\alpha_{1}^{2}-4\alpha_{1}\alpha_{3}+\alpha_{2}^{2}}-\alpha_{2}}}{4\alpha_{1}}}{\alpha_{1}}}{\alpha_{1}}$$

$$\beta_{4} = \frac{\alpha_{1}\sqrt{\frac{2\alpha_{2}\left(\alpha_{2}-\sqrt{8\alpha_{1}^{2}-4\alpha_{1}\alpha_{3}+\alpha_{2}^{2}}\right)-4\alpha_{1}\alpha_{3}}{\alpha_{1}^{2}}-8}+\sqrt{8\alpha_{1}^{2}-4\alpha_{1}\alpha_{3}+\alpha_{2}^{2}}-\alpha_{2}}}{4\alpha_{1}}}{\alpha_{1}}}{\alpha_{1}}$$

The solution gives

$$\beta_1 \beta_2 = 1, \quad \beta_3 \beta_4 = 1.$$
 (A23)

If $l_4 \neq 0$, there is a significant challenge in seeking a comprehensive analytical solution, to which a case-by-case study is necessary. To simplify discussion, we focus on the special case where $l_4=0$. Set $l_4=0$. Eq. (A5) gives

$$(l_2 + m\beta + l_3\beta^2)(l_3 + m\beta + l_2\beta^2) = 0$$
(A24)

Since det B=0 has been discussed, we assume that det $B=l_2l_3\neq 0$. Solutions to Eq. (A24) are

$$\beta_1 = \frac{-m - \sqrt{m^2 - 4l_2 l_3}}{2l_3},\tag{A25a}$$

$$\beta_2 = \frac{-m + \sqrt{m^2 - 4l_2 l_3}}{2l_2},\tag{A25b}$$

$$\beta_3 = \frac{-m + \sqrt{m^2 - 4l_2 l_3}}{2l_3},$$

$$\beta_4 = \frac{-m - \sqrt{m^2 - 4l_2 l_3}}{2l_2}.$$
(A25d)

$$\beta_4 = \frac{-m - \sqrt{m^2 - 4l_2 l_3}}{2l_2}.$$
(A25d)

 eta_1 and eta_3 are solutions to $l_2+meta+l_3eta^2=0$. eta_2 and eta_4 are solutions to $l_3+meta+l_2eta^2=0$. Moreover, $eta_1eta_2=1$ and $eta_3eta_4=1$ hold. It can be easily verified that $|eta_1|=|eta_2|=1$ enforces $|eta_3|=|eta_4|=1$, and vice versa. Therefore, we only need to consider 4 cases:

Case I. $|\beta_1| > 1$, $|\beta_2| < 1$, $|\beta_3| > 1$, $|\beta_4| < 1$.

Case II. $|\beta_1| < 1$, $|\beta_2| > 1$, $|\beta_3| < 1$, $|\beta_4| > 1$.

Case III. $|\beta_1| > 1$, $|\beta_2| < 1$, $|\beta_3| < 1$, $|\beta_4| > 1$.

Case IV. $|\beta_1| < 1$, $|\beta_2| > 1$, $|\beta_3| > 1$, $|\beta_4| < 1$.

Case I $|\beta_1| > 1$, $|\beta_2| < 1$, $|\beta_3| > 1$, $|\beta_4| < 1$.

The boundary bases corresponding to β_2 and β_4 are denoted as \mathbf{w}^2 and \mathbf{w}^4 , respectively.

$$\mathbf{w}^{2} = \begin{pmatrix} \beta_{2}w^{2,a} & \beta_{2}w^{2,b} & \beta_{2}^{2}w^{2,a} & \beta_{2}^{2}w^{2,b} & \cdots & \beta_{2}^{N}w^{2,a} & \beta_{2}^{N}w^{2,b} \end{pmatrix}^{T},
\mathbf{w}^{4} = \begin{pmatrix} \beta_{4}w^{4,a} & \beta_{4}w^{4,b} & \beta_{4}^{2}w^{4,a} & \beta_{4}^{2}w^{4,b} & \cdots & \beta_{4}^{N}w^{4,a} & \beta_{4}^{N}w^{4,b} \end{pmatrix}^{T}.$$

The bulk recurrence relation Eq. (A3) gives

$$\begin{pmatrix} l_1 + n\beta_j + l_1\beta_j^2 & l_2 + m\beta_j + l_3\beta_j^2 \\ 0 & 0 \end{pmatrix} \begin{pmatrix} w^{j,a} \\ w^{j,b} \end{pmatrix} = 0, \quad j = 2, 4.$$
 (A26)

Eq. (A26) is solved by

$$w^{j,a} = l_2 + m\beta_j + l_3\beta_j^2$$
, $w^{j,b} = -(l_1 + n\beta_j + l_1\beta_j^2)$, $j = 2, 4$

A trial solution $\mathbf{u}^{2,4}$

$$\mathbf{u}^{2,4} = c_2 \mathbf{w}^2 + c_4 \mathbf{w}^4 = \begin{pmatrix} u_1^{2,4,A} & u_1^{2,4,B} & u_2^{2,4,A} & u_2^{2,4,B} & \cdots & u_N^{2,4,A} & u_N^{2,4,B} \end{pmatrix}^T$$

is a linear combination of \mathbf{w}^2 and \mathbf{w}^4 .

$$\begin{pmatrix} u_l^{2,4,a} \\ u_l^{2,4,b} \end{pmatrix} = \beta_2^l \begin{pmatrix} l_2 + m\beta_2 + l_3\beta_2^2 \\ -(l_1 + n\beta_2 + l_1\beta_2^2) \end{pmatrix} c_2 + \beta_4^l \begin{pmatrix} l_2 + m\beta_4 + l_3\beta_4^2 \\ -(l_1 + n\beta_4 + l_1\beta_4^2) \end{pmatrix} c_4.$$

We discuss the condition $\beta_2 \neq \beta_4$ at first, which implies $m^2 \neq 4l_1l_2$. Since $|\beta_2| < 1$, $|\beta_4| < 1$, $\mathbf{u}^{2,4}$ is required to satisfy the boundary condition Eq. (A8), which renders

$$\begin{pmatrix} r_1 & r_2 \\ \beta_2^2 l_2 \left(l_2 + \beta_2^2 l_3 + \beta_2 m \right) + \beta_2 m \left(l_2 + \beta_2^2 l_3 + \beta_2 m \right) & \beta_4^2 l_2 \left(l_2 + \beta_4^2 l_3 + \beta_4 m \right) + \beta_4 m \left(l_2 + \beta_4^2 l_3 + \beta_4 m \right) \end{pmatrix} \begin{pmatrix} c_2 \\ c_4 \end{pmatrix} = 0,$$

where

$$r_1 = \beta_2^2 l_1 \left(l_2 + \beta_2^2 l_3 + \beta_2 m \right) + \beta_2^2 l_3 \left(\beta_2^2 (-l_1) - l_1 - \beta_2 n \right) + \beta_2 m \left(\beta_2^2 (-l_1) - l_1 - \beta_2 n \right) + \beta_2 n \left(l_2 + \beta_2^2 l_3 + \beta_2 m \right),$$

$$r_2 = \beta_4^2 l_1 \left(l_2 + \beta_4^2 l_3 + \beta_4 m \right) + \beta_4^2 l_3 \left(\beta_4^2 (-l_1) - l_1 - \beta_4 n \right) + \beta_4 m \left(\beta_4^2 (-l_1) - l_1 - \beta_4 n \right) + \beta_4 n \left(l_2 + \beta_4^2 l_3 + \beta_4 m \right).$$

Nontrivial solution to c_2 , c_4 renders

$$(l_2 - l_3)(n(l_2 + l_3) - 2l_1m) = 0.$$

 $l_2=l_3$ renders either $|\beta_2||\beta_4|=1$ or $|\beta_2|=|\beta_4|=1$, contradicting the assumption that $|\beta_2|<1, |\beta_4|<1$. Therefore, if $n(l_2+l_3)=2l_1m$, there exists a boundary zero mode satisfying boundary condition Eq. (A8). The above discussion has ignored $m^2=4l_2l_3$. The condition for nontrivial solution to boundary condition Eq. (A8) enforces $|\beta_2|=|\beta_4|=1$, contradicting $|\beta_2|<1, |\beta_4|<1$.

The next step is the discussion on the boundary bases \mathbf{w}^1 and \mathbf{w}^3 corresponding to β_1 and β_3 , respectively.

$$\mathbf{w}^{1} = \begin{pmatrix} \beta_{1}w^{1,a} & \beta_{1}w^{1,b} & \beta_{1}^{2}w^{1,a} & \beta_{1}^{2}w^{1,b} & \cdots & \beta_{1}^{N}w^{1,a} & \beta_{1}^{N}w^{1,b} \end{pmatrix}^{T},
\mathbf{w}^{3} = \begin{pmatrix} \beta_{3}w^{3,a} & \beta_{3}w^{3,b} & \beta_{3}^{2}w^{3,a} & \beta_{3}^{2}w^{3,b} & \cdots & \beta_{3}^{N}w^{3,a} & \beta_{3}^{N}w^{3,b} \end{pmatrix}^{T}.$$

The bulk recurrence relation Eq. (A3) gives

$$\begin{pmatrix} l_1 + n\beta_j + l_1\beta_j^2 & 0\\ l_3 + m\beta_j + l_2\beta_j^2 & 0 \end{pmatrix} \begin{pmatrix} w^{j,a} \\ w^{j,b} \end{pmatrix} = 0, \quad j = 1,3$$
 (A27)

Eq. (A27) is solved by

$$w^{j,a} = 0, \quad w^{j,b} = 1, \quad j = 1, 3.$$

A trial solution $\mathbf{u}^{1,3}$ is a linear combination of \mathbf{w}^1 and \mathbf{w}^3 .

$$\mathbf{u}^{1,3} = c_1 \mathbf{w}^1 + c_3 \mathbf{w}^3 = \begin{pmatrix} u_1^{1,3,a} & u_1^{1,3,b} & u_2^{1,3,a} & u_2^{1,3,b} & \cdots & u_N^{1,3,a} & u_N^{1,3,b} \end{pmatrix}^T,$$

where

$$\begin{pmatrix} u_l^{1,3,a} \\ u_l^{1,3,b} \end{pmatrix} = \beta_1^l \begin{pmatrix} 0 \\ 1 \end{pmatrix} c_1 + \beta_3^l \begin{pmatrix} 0 \\ 1 \end{pmatrix} c_3.$$

 $\beta_1 \neq \beta_3$ is discussed in the first step, which implies $m^2 \neq 4l_1l_2$. Since $|\beta_1| > 1$, $|\beta_3| > 1$, $\mathbf{u}^{1,3}$ is required to satisfy the boundary condition Eq. (A9), rendering

$$\begin{pmatrix} \beta_1^{N-1}(l_2 + \beta_1 m) & \beta_3^{N-1}(l_2 + \beta_3 m) \\ 0 & 0 \end{pmatrix} \begin{pmatrix} c_1 \\ c_3 \end{pmatrix} = 0$$
 (A28)

Eq. (A28) always has a nontrivial solution

$$c_1 = \beta_3^{N-1}(l_2 + \beta_3 m)c, \quad c_3 = -\beta_1^{N-1}(l_2 + \beta_1 m)c,$$

where c is a normalization constant. Therefore, there always exist boundary states satisfying the boundary condition Eq. (A9). If $m^2 = 4l_2l_3$, $\beta_1 = \beta_3 = \frac{-m}{2l_3}$. The condition for nontrivial solution to boundary condition Eq. (A9) enforces $|\beta_1| = |\beta_3| = 1$, contradicting $|\beta_1| > 1$, $|\beta_3| > 1$.

Case II $|\beta_1| < 1, |\beta_2| > 1, |\beta_3| < 1, |\beta_4| > 1.$

Denote the boundary bases corresponding to β_1 and β_3 as \mathbf{w}^1 and \mathbf{w}^3 , respectively.

$$\mathbf{w}^{1} = (\beta_{1}w^{1,a} \ \beta_{1}w^{1,b} \ \beta_{1}^{2}w^{1,a} \ \beta_{1}^{2}w^{1,b} \ \cdots \ \beta_{1}^{N}w^{1,a} \ \beta_{1}^{N}w^{1,b})^{T},$$

$$\mathbf{w}^{3} = (\beta_{3}w^{3,a} \ \beta_{3}w^{3,b} \ \beta_{3}^{2}w^{3,a} \ \beta_{3}^{2}w^{3,b} \ \cdots \ \beta_{3}^{N}w^{3,a} \ \beta_{3}^{N}w^{3,b})^{T}.$$

The bulk recurrence relation Eq. (A3) gives

$$\begin{pmatrix} l_1 + n\beta_j + l_1\beta_j^2 & 0 \\ l_3 + m\beta_j + l_2\beta_j^2 & 0 \end{pmatrix} \begin{pmatrix} w^{j,a} \\ w^{j,b} \end{pmatrix} = 0, \quad j = 1, 3.$$
 (A29)

Eq. (A29) is solved by

$$w^{j,a} = 0, \quad w^{j,b} = 1, \quad j = 1,3.$$
 (A30)

A trial solution $\mathbf{u}^{1,3}$ is a linear combination of \mathbf{w}^1 and \mathbf{w}^3 .

$$\mathbf{u}^{1,3} = c_1 \mathbf{w}^1 + c_3 \mathbf{w}^3 = \begin{pmatrix} u_1^{1,3,a} & u_1^{1,3,b} & u_2^{1,3,a} & u_2^{1,3,b} & \cdots & u_N^{1,3,a} & u_N^{1,3,b} \end{pmatrix}^T,$$

where

$$\begin{pmatrix} u_l^{1,3,a} \\ u_l^{1,3,b} \end{pmatrix} = \beta_1^l \begin{pmatrix} 0 \\ 1 \end{pmatrix} c_1 + \beta_3^l \begin{pmatrix} 0 \\ 1 \end{pmatrix} c_3.$$
 (A31)

 $\beta_1 \neq \beta_3 \Leftrightarrow m^2 \neq 4l_2l_3$ is discussed at first. Since $|\beta_1| < 1$, $|\beta_3| < 1$, $\mathbf{u}^{1,3}$ is required to satisfy the boundary condition Eq. (A8), which renders

$$\begin{pmatrix} \beta_1(\beta_1 l_3 + m) & \beta_3(\beta_3 l_3 + m) \\ 0 & 0 \end{pmatrix} \begin{pmatrix} c_1 \\ c_3 \end{pmatrix} = 0.$$
 (A32)

Eq. (A32) always has nontrivial solutions to c_1 and c_3 .

$$c_1 = -\beta_3(\beta_3 l_3 + m)c, \quad c_3 = \beta_1(\beta_1 l_3 + m)c,$$
 (A33)

where c is a normalization constant. Therefore, there always exist boundary states satisfying the boundary condition Eq. (A8). If $m^2 = 4l_2l_3$, $\beta_1 = \beta_3 = \frac{-m}{2l_3}$, the condition for nontrivial solution to boundary condition Eq. (A8) enforces $|\beta_1| = |\beta_3| = 1$, contradicting $|\beta_1| < 1$, $|\beta_3| < 1$.

The boundary bases corresponding to β_2 and β_4 are \mathbf{w}^2 and \mathbf{w}^4 , given by

$$\mathbf{w}^{2} = (\beta_{2}w^{2,a} \ \beta_{2}w^{2,b} \ \beta_{2}^{2}w^{2,a} \ \beta_{2}^{2}w^{2,b} \ \cdots \ \beta_{2}^{N}w^{2,a} \ \beta_{2}^{N}w^{2,b})^{T},$$

$$\mathbf{w}^{4} = (\beta_{4}w^{4,a} \ \beta_{4}w^{4,b} \ \beta_{4}^{2}w^{4,a} \ \beta_{4}^{2}w^{4,b} \ \cdots \ \beta_{4}^{N}w^{4,a} \ \beta_{4}^{N}w^{4,b})^{T}.$$

The bulk recurrence relation Eq. (A3) gives

$$\begin{pmatrix} l_1 + n\beta_j + l_1\beta_j^2 & l_2 + m\beta_j + l_3\beta_j^2 \\ 0 & 0 \end{pmatrix} \begin{pmatrix} w^{j,a} \\ w^{j,b} \end{pmatrix} = 0, \quad j = 2, 4,$$

which is solved by

$$w^{j,a} = l_2 + m\beta_j + l_3\beta_j^2, \quad w^{j,b} = -(l_1 + n\beta_j + l_1\beta_j^2).$$

A trial solution $\mathbf{u}^{2,4}$ is a linear combination of \mathbf{w}^2 and \mathbf{w}^4 .

$$\mathbf{u}^{2,4} = c_2 \mathbf{w}^2 + c_4 \mathbf{w}^4 = \begin{pmatrix} u_1^{2,4,a} & u_1^{2,4,b} & u_2^{2,4,a} & u_2^{2,4,b} & \cdots & u_N^{2,4,a} & u_N^{2,4,b} \end{pmatrix}^T,$$

where

$$\begin{pmatrix} u_l^{2,4,a} \\ u_l^{2,4,b} \end{pmatrix} = \beta_2^l \begin{pmatrix} l_2 + m\beta_2 + l_3\beta_2^2 \\ -(l_1 + n\beta_2 + l_1\beta_2^2) \end{pmatrix} c_2 + \beta_4^l \begin{pmatrix} l_2 + m\beta_4 + l_3\beta_4^2 \\ -(l_1 + n\beta_4 + l_1\beta_4^2) \end{pmatrix} c_4.$$

Since $|\beta_2| > 1$, $|\beta_4| > 1$, $\mathbf{u}^{2,4}$ is required to satisfy the boundary condition Eq. (A9). If $\beta_2 \neq \beta_4$, i.e., $m^2 \neq 4l_1l_2$, nontrivial solution to the boundary condition Eq. (A9) renders

$$(l_2 - l_3)(n(l_2 + l_3) - 2l_1m) = 0.$$

Therefore, if $n(l_2 + l_3) = 2l_1m$, there exists a boundary zero mode $\mathbf{u}^{2,4}$ satisfying the boundary condition Eq. (A9). $l_2 = l_3$ renders $|\beta_2| = |\beta_4| = 1$ or $|\beta_2| |\beta_4| = 1$, contradicting the assumption that $|\beta_2| > 1$, $|\beta_4| > 1$. If $m^2 = 4l_2l_3$, $\beta_2 = \beta_4 = \frac{-m}{2l_2}$, the condition for nontrivial solution to boundary condition Eq. (A9) enforces $|\beta_2| = |\beta_4| = 1$, contradicting $|\beta_2| > 1$, $|\beta_4| > 1$.

Case III $|\beta_1| > 1$, $|\beta_2| < 1$, $|\beta_3| < 1$, $|\beta_4| > 1$.

The boundary bases corresponding to β_2 and β_3 are denoted as \mathbf{w}^2 and \mathbf{w}^3 , respectively.

$$\mathbf{w}^{2} = \begin{pmatrix} \beta_{2}w^{2,a} & \beta_{2}w^{2,b} & \beta_{2}^{2}w^{2,a} & \beta_{2}^{2}w^{2,b} & \cdots & \beta_{2}^{N}w^{2,a} & \beta_{2}^{N}w^{2,b} \end{pmatrix}^{T},$$

$$\mathbf{w}^{3} = \begin{pmatrix} \beta_{3}w^{3,a} & \beta_{3}w^{3,b} & \beta_{3}^{2}w^{3,a} & \beta_{3}^{2}w^{3,b} & \cdots & \beta_{3}^{N}w^{3,a} & \beta_{3}^{N}w^{3,b} \end{pmatrix}^{T}.$$

The bulk recurrence relation Eq. (A3) gives

$$\begin{pmatrix} l_1 + n\beta_2 + l_1\beta_2^2 & l_2 + m\beta_2 + l_3\beta_2^2 \\ 0 & 0 \end{pmatrix} \begin{pmatrix} w^{2,a} \\ w^{2,b} \end{pmatrix} = 0, \quad \begin{pmatrix} l_1 + n\beta_3 + l_1\beta_3^2 & 0 \\ l_3 + m\beta_3 + l_2\beta_3^2 & 0 \end{pmatrix} \begin{pmatrix} w^{3,a} \\ w^{3,b} \end{pmatrix} = 0.$$
 (A34)

The solution to Eq. (A34) is given by

$$\begin{cases} w^{2,a} = l_2 + m\beta_2 + l_3\beta_2^2 \\ w^{2,b} = -(l_1 + n\beta_2 + l_1\beta_2^2) \end{cases}, \begin{cases} w^{3,a} = 0 \\ w^{3,b} = 1 \end{cases}.$$

A trial solution $\mathbf{u}^{2,3}$ is a linear combination of \mathbf{w}^2 and \mathbf{w}^3

$$\mathbf{u}^{2,3} = c_2 \mathbf{w}^2 + c_3 \mathbf{w}^3 = \begin{pmatrix} u_1^{2,3,A} & u_1^{2,3,B} & u_2^{2,3,A} & u_2^{2,3,B} & \cdots & u_N^{2,3,A} & u_N^{2,3,B} \end{pmatrix}^T,$$

where

$$\begin{pmatrix} u_l^{2,3,a} \\ u_l^{2,3,b} \end{pmatrix} = \beta_2^l \begin{pmatrix} l_2 + m\beta_2 + l_3\beta_2^2 \\ -(l_1 + n\beta_2 + l_1\beta_2^2) \end{pmatrix} c_2 + \beta_3^l \begin{pmatrix} 0 \\ 1 \end{pmatrix} c_3.$$

Since $|\beta_2| < 1$, $|\beta_3| < 1$, $\mathbf{u}^{2,3}$ is required to satisfy the boundary condition specified by Eq. (A8). If $\beta_2 \neq \beta_3 \Leftrightarrow l_2 \neq l_3$, the boundary condition Eq. (A8) renders

$$\begin{pmatrix} \beta_2 l_2 n - \beta_2 l_1 (\beta_2 (l_3 - l_2) + m) & \beta_3 (\beta_3 l_3 + m) \\ \beta_2 (\beta_2 l_2 + m) (l_2 + \beta_2 (\beta_2 l_3 + m)) & 0 \end{pmatrix} \begin{pmatrix} c_2 \\ c_3 \end{pmatrix} = 0.$$
 (A35)

Nontrivial solution to Eq. (A35) implies

$$\det \begin{pmatrix} \beta_2 l_2 n - \beta_2 l_1 (\beta_2 (l_3 - l_2) + m) & \beta_3 (\beta_3 l_3 + m) \\ \beta_2 (\beta_2 l_2 + m) (l_2 + \beta_2 (\beta_2 l_3 + m)) & 0 \end{pmatrix} = 0.$$
(A36)

Eq. (A36) together with Eq. (A25b), Eq. (A25c) renders

$$2ml_2\beta_2 + 2l_2(l_2 + l_3) = 2ml_3\beta_3 + 2l_2(l_2 + l_3) = 0, (A37)$$

Eq. (A37) together with Eq. (A25b) and Eq. (A25c) enforces $\beta_2=1$, $\beta_3=l_2/l_3$, which contradicts our assumption $|\beta_2|<1$, $|\beta_3|<1$. If $\beta_2=\beta_3\Leftrightarrow l_2=l_3$, a legitimate solution $\mathbf{u}^{2,3}$ satisfying the boundary condition Eq. (A8) does not exist either. The next step is to discuss the boundary bases corresponding to β_1 and β_4 , which are denoted as \mathbf{w}^1 and \mathbf{w}^4 , respectively.

$$\mathbf{w}^{1} = \begin{pmatrix} \beta_{1}w^{1,a} & \beta_{1}w^{1,b} & \beta_{1}^{2}w^{1,a} & \beta_{1}^{2}w^{1,b} & \cdots & \beta_{1}^{N}w^{1,a} & \beta_{1}^{N}w^{1,b} \end{pmatrix}^{T},
\mathbf{w}^{4} = \begin{pmatrix} \beta_{4}w^{4,a} & \beta_{4}w^{4,b} & \beta_{4}^{2}w^{4,a} & \beta_{4}^{2}w^{4,b} & \cdots & \beta_{4}^{N}w^{4,a} & \beta_{4}^{N}w^{4,b} \end{pmatrix}^{T}.$$

The bulk recurrence relation Eq. (A3) gives

$$\begin{pmatrix} l_1 + n\beta_1 + l_1\beta_1^2 & 0 \\ l_3 + m\beta_1 + l_2\beta_1^2 & 0 \end{pmatrix} \begin{pmatrix} w^{1,a} \\ w^{1,b} \end{pmatrix} = 0, \quad \begin{pmatrix} l_1 + n\beta_4 + l_1\beta_4^2 & l_2 + m\beta_4 + l_3\beta_4^2 \\ 0 & 0 \end{pmatrix} \begin{pmatrix} w^{4,a} \\ w^{4,b} \end{pmatrix} = 0.$$
 (A38)

Eq. (A38) is solved by

$$\begin{cases} w^{1,a} = 0 \\ w^{1,b} = 1 \end{cases}, \begin{cases} w^{4,a} = l_2 + m\beta_4 + l_3\beta_4^2 \\ w^{4,b} = -(l_1 + n\beta_4 + l_1\beta_4^2) \end{cases}.$$

A trial solution $\mathbf{u}^{1,4}$ is a linear combination of \mathbf{w}^1 and \mathbf{w}^4 .

$$\mathbf{u}^{1,4} = c_1 \mathbf{w}^1 + c_4 \mathbf{w}^4 = \begin{pmatrix} u_1^{1,4,a} & u_1^{1,4,b} & u_2^{1,4,a} & u_2^{1,4,b} & \cdots & u_N^{1,4,a} & u_N^{1,4,b} \end{pmatrix}^T,$$

where

$$\begin{pmatrix} u_l^{1,4,a} \\ u_l^{1,4,b} \end{pmatrix} = \beta_1^l \begin{pmatrix} 0 \\ 1 \end{pmatrix} c_1 + \beta_4^l \begin{pmatrix} l_2 + m\beta_4 + l_3\beta_4^2 \\ -(l_1 + n\beta_4 + l_1\beta_4^2) \end{pmatrix} c_4.$$

Since $|\beta_1| > 1$, $|\beta_4| > 1$, $\mathbf{u}^{1,4}$ is required to satisfy the boundary condition Eq. (A8). If $\beta_2 \neq \beta_3 \Leftrightarrow l_2 \neq l_3$, the boundary condition Eq. (A9) renders

$$\begin{pmatrix} \beta_1^{N-1}(l_2+\beta_1 m) & \beta_4^{N+1}(\beta_4 l_3 n - l_1(l_2 - l_3 + \beta_4 m)) \\ 0 & \beta_4^{N-1}(l_3 + \beta_4 m)(l_2 + \beta_4(\beta_4 l_3 + m)) \end{pmatrix} \begin{pmatrix} c_1 \\ c_4 \end{pmatrix} = 0.$$
 (A39)

Nontrivial solution to Eq. (A39) implies

$$\det \begin{pmatrix} \beta_1^{N-1}(l_2 + \beta_1 m) & \beta_4^{N+1}(\beta_4 l_3 n - l_1(l_2 - l_3 + \beta_4 m)) \\ 0 & \beta_4^{N-1}(l_3 + \beta_4 m)(l_2 + \beta_4(\beta_4 l_3 + m)) \end{pmatrix} = 0.$$
 (A40)

Eq. (A40) together with Eq. (A25a), Eq. (A25d) renders

$$2ml_2\beta_4 + 2l_2(l_2 + l_3) = 2ml_3\beta_1 + 2l_2(l_2 + l_3) = 0.$$
(A41)

Eq. (A41) together with Eq. (A25a) and Eq. (A25d) enforces $\beta_4=1$, $\beta_1=l_2/l_3$, which contradicts our assumption $|\beta_1|>1$, $|\beta_4|>1$. If $\beta_1=\beta_4\Leftrightarrow l_2=l_3$, a legitimate solution $\mathbf{u}^{1,4}$ satisfying the boundary condition Eq. (A9) does not exist either.

Case IV $|\beta_1| < 1, |\beta_2| > 1, |\beta_3| > 1, |\beta_4| < 1.$

Denote the boundary bases corresponding to β_1 and β_4 as \mathbf{w}^1 and \mathbf{w}^4 , respectively.

$$\mathbf{w}^{1} = \begin{pmatrix} \beta_{1}w^{1,a} & \beta_{1}w^{1,b} & \beta_{1}^{2}w^{1,a} & \beta_{1}^{2}w^{1,b} & \cdots & \beta_{1}^{N}w^{1,a} & \beta_{1}^{N}w^{1,b} \end{pmatrix}^{T},$$

$$\mathbf{w}^{4} = \begin{pmatrix} \beta_{4}w^{4,a} & \beta_{4}w^{4,b} & \beta_{4}^{2}w^{4,a} & \beta_{4}^{2}w^{4,b} & \cdots & \beta_{4}^{N}w^{4,a} & \beta_{4}^{N}w^{4,b} \end{pmatrix}^{T}.$$

The bulk recurrence relation Eq. (A3) gives

$$\begin{pmatrix} l_1 + n\beta_1 + l_1\beta_1^2 & 0 \\ l_3 + m\beta_1 + l_2\beta_1^2 & 0 \end{pmatrix} \begin{pmatrix} w^{1,a} \\ w^{1,b} \end{pmatrix} = 0, \quad \begin{pmatrix} l_1 + n\beta_4 + l_1\beta_4^2 & l_2 + m\beta_4 + l_3\beta_4^2 \\ 0 & 0 \end{pmatrix} \begin{pmatrix} w^{4,a} \\ w^{4,b} \end{pmatrix} = 0.$$
 (A42)

Eq. (A42) is solved by

$$\begin{cases} w^{1,a} = 0 \\ w^{1,b} = 1 \end{cases}, \begin{cases} w^{4,a} = l_2 + m\beta_4 + l_3\beta_4^2 \\ w^{4,b} = -(l_1 + n\beta_4 + l_1\beta_4^2) \end{cases}.$$

A trial solution is a linear combination of \mathbf{w}^1 and \mathbf{w}^4 .

$$\mathbf{u}^{1,4} = c_1 \mathbf{w}^1 + c_4 \mathbf{w}^4 = \begin{pmatrix} u_1^{1,4,A} & u_1^{1,4,B} & u_2^{1,4,A} & u_2^{1,4,B} & \cdots & u_N^{1,4,A} & u_N^{1,4,B} \end{pmatrix}^T,$$

where

$$\begin{pmatrix} u_l^{1,4,A} \\ u_l^{1,4,B} \end{pmatrix} = \beta_1^l \begin{pmatrix} 0 \\ 1 \end{pmatrix} c_1 + \beta_4^l \begin{pmatrix} l_2 + m\beta_4 + l_3\beta_4^2 \\ -(l_1 + n\beta_4 + l_1\beta_4^2) \end{pmatrix} c_4.$$

Since $|\beta_1| < 1$, $|\beta_4| < 1$, $\mathbf{u}^{1,4}$ is required to satisfy the boundary condition specified by Eq. (A8). If $\beta_1 \neq \beta_4 \Leftrightarrow l_2 \neq l_3$, the boundary condition Eq. (A8) renders

$$\begin{pmatrix} \beta_1(\beta_1 l_3 + m) & \beta_4(l_2 n - l_1(\beta_4(l_3 - l_2) + m)) \\ 0 & \beta_4(\beta_4 l_2 + m)(l_2 + \beta_4(\beta_4 l_3 + m)) \end{pmatrix} \begin{pmatrix} c_1 \\ c_4 \end{pmatrix} = 0.$$
(A43)

Nontrivial solution to Eq. (A43) requires

$$\det \begin{pmatrix} \beta_1(\beta_1 l_3 + m) & \beta_4(l_2 n - l_1(\beta_4(l_3 - l_2) + m)) \\ 0 & \beta_4(\beta_4 l_2 + m)(l_2 + \beta_4(\beta_4 l_3 + m)) \end{pmatrix} = 0.$$
 (A44)

Eq. (A44) along with Eq. (A25a) and Eq. (A25d) renders

$$2ml_2\beta_4 + 2l_2(l_2 + l_3) = 2ml_3\beta_1 + 2l_2(l_2 + l_3) = 0.$$
(A45)

Eq. (A45), Eq. (A25a) and Eq. (A25d) enforce $\beta_4 = 1$, $\beta_1 = l_3/l_2$, which contradicts our assumption $|\beta_1| < 1$, $|\beta_4| < 1$. If $\beta_1 = \beta_4 \Leftrightarrow l_2 = l_3$, a legitimate solution $\mathbf{u}^{1,4}$ satisfying the boundary condition Eq. (A8) does not exist either.

The next step is to discuss the boundary bases \mathbf{w}^2 and \mathbf{w}^3 corresponding to β_2 and β_3 as, respectively.

$$\mathbf{w}^{2} = \begin{pmatrix} \beta_{2}w^{2,a} & \beta_{2}w^{2,b} & \beta_{2}^{2}w^{2,a} & \beta_{2}^{2}w^{2,b} & \cdots & \beta_{2}^{N}w^{2,a} & \beta_{2}^{N}w^{2,b} \end{pmatrix}^{T},
\mathbf{w}^{3} = \begin{pmatrix} \beta_{3}w^{3,a} & \beta_{3}w^{3,b} & \beta_{3}^{2}w^{3,a} & \beta_{3}^{2}w^{3,b} & \cdots & \beta_{3}^{N}w^{3,a} & \beta_{3}^{N}w^{3,b} \end{pmatrix}^{T}.$$

The bulk recurrence relation Eq. (A3) gives

$$\begin{pmatrix} l_1 + n\beta_2 + l_1\beta_2^2 & l_2 + m\beta_2 + l_3\beta_2^2 \\ 0 & 0 \end{pmatrix} \begin{pmatrix} w^{2,a} \\ w^{2,b} \end{pmatrix} = 0, \quad \begin{pmatrix} l_1 + n\beta_3 + l_1\beta_3^2 & 0 \\ l_3 + m\beta_3 + l_2\beta_3^2 & 0 \end{pmatrix} \begin{pmatrix} w^{3,a} \\ w^{3,b} \end{pmatrix} = 0.$$
 (A46)

Eq. (A46) is solved by

$$\begin{cases} w^{2,a} = l_2 + m\beta_2 + l_3\beta_2^2 \\ w^{2,b} = -(l_1 + n\beta_2 + l_1\beta_2^2) \end{cases}, \begin{cases} w^{3,a} = 0 \\ w^{3,b} = 1 \end{cases}.$$

A trial solution is a linear combination of \mathbf{w}^2 and \mathbf{w}^3 .

$$\mathbf{u}^{2,3} = c_2 \mathbf{w}^2 + c_3 \mathbf{w}^3 = \begin{pmatrix} u_1^{2,3,a} & u_1^{2,3,b} & u_2^{2,3,a} & u_2^{2,3,b} & \cdots & u_N^{2,3,a} & u_N^{2,3,} \end{pmatrix}^T,$$

where

$$\begin{pmatrix} u_l^{2,3,a} \\ u_l^{2,3,b} \end{pmatrix} = \beta_2^l \begin{pmatrix} l_2 + m\beta_2 + l_3\beta_2^2 \\ -(l_1 + n\beta_2 + l_1\beta_2^2) \end{pmatrix} c_2 + \beta_3^l \begin{pmatrix} 0 \\ 1 \end{pmatrix} c_3$$
 (A47)

Since $|\beta_2| > 1$, $|\beta_3| > 1$, $\mathbf{u}^{2,3}$ is required to satisfy the boundary condition specified by Eq. (A9). If $\beta_2 \neq \beta_3 \Leftrightarrow l_2 \neq l_3$, the boundary condition (A9) renders

$$\begin{pmatrix} \beta_2^{N+1}(\beta_2 l_3 n - l_1(l_2 - l_3 + \beta_2 m)) & \beta_3^{N-1}(l_2 + \beta_3 m) \\ \beta_2^{N-1}(l_3 + \beta_2 m)(l_2 + \beta_2(\beta_2 l_3 + m)) & 0 \end{pmatrix} \begin{pmatrix} c_2 \\ c_3 \end{pmatrix} = 0$$
 (A48)

Nontrivial solution to Eq. (A48) requires

$$\det \begin{pmatrix} \beta_2^{N+1}(\beta_2 l_3 n - l_1(l_2 - l_3 + \beta_2 m)) & \beta_3^{N-1}(l_2 + \beta_3 m) \\ \beta_2^{N-1}(l_3 + \beta_2 m)(l_2 + \beta_2(\beta_2 l_3 + m)) & 0 \end{pmatrix} = 0.$$
(A49)

Eq. (A49), Eq. (A25b) and Eq. (A25c) give

$$2ml_2\beta_2 + 2l_2(l_2 + l_3) = 2ml_3\beta_3 + 2l_2(l_2 + l_3) = 0.$$
(A50)

Eq. (A50), Eq. (A25b) and Eq. (A25c) enforce $\beta_2 = 1$, $\beta_3 = l_3/l_2$, which contradicts our assumption $|\beta_2| > 1$, $|\beta_3| > 1$. If $\beta_2 = \beta_3 \Leftrightarrow l_2 = l_3$, it is easy to verify that a legitimate boundary zero mode satisfying the boundary condition Eq. (A9) does not exist either.

 $|\beta_1| > 1, \ |\beta_2| < 1, \ |\beta_3| > 1, \ |\beta_4| < 1 \ \text{and} \ |\beta_1| < 1, \ |\beta_2| > 1, \ |\beta_3| < 1, \ |\beta_4| > 1 \ \text{can} \ \text{be summarized into the condition}$ $|m| < |l_2 + l_3|. \ \text{If} \ \left\{ \begin{array}{l} |m| < |l_2 + l_3| \\ |l_3| < |l_2| \end{array} \right. \text{, the discussion falls in Case II.} \ \text{If} \ \left\{ \begin{array}{l} |m| < |l_2 + l_3| \\ |l_2| < |l_3| \end{array} \right. \text{, the discussion falls in Case II.}$

In summary, if

$$\begin{cases} l_4 = 0, \\ n(l_2 + l_3) \neq 2l_1 m, & l_2 \neq l_3, \quad l_2 l_3 \neq 0, \\ |m| < |l_2 + l_3|, & \end{cases}$$

the K-matrix Eq. (2) has one boundary zero mode. More specifically, if $|l_2| < |l_3|$, the boundary zero mode is a lower boundary zero mode, satisfying the boundary condition Eq. (A8). If $|l_2| > |l_3|$, the boundary zero mode is an upper boundary zero mode, satisfying the boundary condition Eq. (A9). If

$$\begin{cases} l_4 = 0, & n(l_2 + l_3) = 2l_1 m, \\ l_2 \neq l_3, & l_2 l_3 \neq 0, \\ |m| < |l_2 + l_3|, \end{cases}$$

the K-matrix Eq. (2) has two boundary zero modes.

- of Condensed Matter Physics 10, 295 (2019).
- [3] S. Vijay, J. Haah, and L. Fu, Fracton topological order, generalized lattice gauge theory, and duality, Physical Review B 94, 235157 (2016).
- [4] J. Haah, Local stabilizer codes in three dimensions without string logical operators, Physical Review A 83, 042330 (2011).
- [5] W. Shirley, K. Slagle, Z. Wang, and X. Chen, Fracton models on general three-dimensional manifolds, Physical Review X 8, 031051 (2018).
- [6] M.-Y. Li and P. Ye, Hierarchy of entanglement renormalization and long-range entangled states, Physical Review B 107, 115169 (2023).
- [7] M.-Y. Li and P. Ye, Fracton physics of spatially extended excitations, Physical Review B **101**, 245134 (2020).
- [8] M.-Y. Li and P. Ye, Fracton physics of spatially extended excitations. ii. polynomial ground state degeneracy of exactly solvable models, Physical Review B 104, 235127 (2021).
- [9] X. Ma, W. Shirley, M. Cheng, M. Levin, J. McGreevy, and X. Chen, Fractonic order in infinite-component Chern-Simons gauge theories, Physical Review B 105 (2022).
- [10] X. Chen, H. T. Lam, and X. Ma, Gapless infinite-component Chern-Simons-Maxwell theories (2022), arXiv:2211.10458 [cond-mat.str-el].
- [11] X. Chen, H. T. Lam, and X. Ma, Ground state degeneracy of infinite-component Chern-Simons-Maxwell theories (2023), arXiv:2306.00291 [cond-mat.str-el].
- [12] X. Wu and Y. Zhang, Two-dimension to three-dimension transition of chiral spin liquid and fractional quantum hall phases (2023), arXiv:2307.06366 [cond-mat.str-el].
- [13] J. Sullivan, A. Dua, and M. Cheng, Weak symmetry breaking and topological order in a 3d compressible quantum liquid (2021), arXiv:2109.13267 [cond-mat.str-el].
- [14] J. Sullivan, T. Iadecola, and D. J. Williamson, Planar p-string condensation: Chiral fracton phases from fractional quantum hall layers and beyond, Phys. Rev. B 103, 205301 (2021).
- [15] X. G. Wen and A. Zee, Classification of abelian quantum hall states and matrix formulation of topological fluids, Phys. Rev. B 46, 2290 (1992).
- [16] Y.-M. Lu and A. Vishwanath, Theory and classification of interacting integer topological phases in two dimensions: A Chern-Simons approach, Phys. Rev. B 86, 125119 (2012).
- [17] Y.-M. Lu and A. Vishwanath, Classification and properties of symmetry-enriched topological phases: Chern-Simons approach with applications to Z_2 spin liquids, Phys. Rev. B 93, 155121 (2016).
- [18] P. Ye and X.-G. Wen, Projective construction of twodimensional symmetry-protected topological phases with u(1), so(3), or su(2) symmetries, Phys. Rev. B 87, 195128 (2013).
- [19] Z.-X. Liu, J.-W. Mei, P. Ye, and X.-G. Wen, $u(1) \times u(1)$ symmetry-protected topological order in gutzwiller wave functions, Phys. Rev. B **90**, 235146 (2014).
- [20] L.-Y. Hung and Y. Wan, K matrix construction of symmetryenriched phases of matter, Phys. Rev. B 87, 195103 (2013).
- [21] Z.-C. Gu, J. C. Wang, and X.-G. Wen, Multikink topological terms and charge-binding domain-wall condensation induced symmetry-protected topological states: Beyond chern-simons/bf field theories, Phys. Rev. B 93, 115136 (2016).
- [22] M. Cheng and Z.-C. Gu, Topological response theory of abelian symmetry-protected topological phases in two dimensions, Phys. Rev. Lett. 112, 141602 (2014).
- [23] L. Balents and M. P. Fisher, Chiral surface states in the bulk quantum hall effect, Physical review letters 76, 2782 (1996).
- [24] C. L. Kane and M. P. A. Fisher, Impurity scattering and transport of fractional quantum hall edge states, Phys. Rev. B 51,

- 13449 (1995).
- [25] J. D. Naud, L. P. Pryadko, and S. L. Sondhi, Fractional quantum hall effect in infinite-layer systems, Phys. Rev. Lett. 85, 5408 (2000).
- [26] J. Naud, L. P. Pryadko, and S. Sondhi, Notes on infinite layer quantum hall systems, Nuclear Physics B 594, 713 (2001).
- [27] D. P. Druist, P. J. Turley, K. D. Maranowski, E. G. Gwinn, and A. C. Gossard, Observation of chiral surface states in the integer quantum hall effect, Phys. Rev. Lett. 80, 365 (1998).
- [28] X. Qiu, R. Joynt, and A. MacDonald, Phases of the multiple quantum well in a strong magnetic field: Possibility of irrational charge, Physical Review B 40, 11943 (1989).
- [29] C. H. Lee and P. Ye, Free-fermion entanglement spectrum through wannier interpolation, Physical Review B 91, 085119 (2015).
- [30] G. Meurant, A review on the inverse of symmetric tridiagonal and block tridiagonal matrices, SIAM Journal on Matrix Analysis and Applications 13, 707 (1992).
- [31] J. I. I. Hirschman, Matrix-valued Toeplitz operators, Duke Mathematical Journal 34, 403 (1967).
- [32] S.-E. Ekström and S. Serra-Capizzano, Eigenvalues and eigenvectors of banded toeplitz matrices and the related symbols, Numerical Linear Algebra with Applications 25, e2137 (2018).
- [33] M. Wax and T. Kailath, Efficient inversion of toeplitz-block toeplitz matrix, IEEE transactions on acoustics, speech, and signal processing 31, 1218 (1983).
- [34] J. Gutiérrez-Gutiérrez, P. M. Crespo, et al., Block toeplitz matrices: Asymptotic results and applications, Foundations and Trends® in Communications and Information Theory 8, 179 (2012).
- [35] G. Heinig and K. Rost, *Algebraic methods for Toeplitz-like matrices and operators*, Vol. 13 (Birkhäuser Basel, 1984).
- [36] W. P. Su, J. R. Schrieffer, and A. J. Heeger, Soliton excitations in polyacetylene, Phys. Rev. B 22, 2099 (1980).
- [37] X.-L. Qi and S.-C. Zhang, Topological insulators and superconductors, Rev. Mod. Phys. 83, 1057 (2011).
- [38] H.-M. Guo, A brief review on one-dimensional topological insulators and superconductors, Science China Physics, Mechanics & Astronomy 59, 1 (2016).
- [39] A. Y. Kitaev, Unpaired Majorana fermions in quantum wires, Physics-Uspekhi 44, 131–136 (2001).
- [40] S.-Q. Shen, *Topological insulators*, Vol. 174 (Springer, 2012).
- [41] J. K. Asbóth, L. Oroszlány, and A. Pályi, A short course on topological insulators, Vol. 919 (Springer, 2016) p. 166.
- [42] R. Movassagh, G. Strang, Y. Tsuji, and R. Hoffmann, The green's function for the Hückel (tight binding) model, Journal of Mathematical Physics 58 (2017).
- [43] B. Blok and X. G. Wen, Effective theories of the fractional quantum hall effect at generic filling fractions, Phys. Rev. B 42, 8133 (1990).
- [44] B. Blok and X. G. Wen, Effective theories of the fractional quantum hall effect: Hierarchy construction, Phys. Rev. B 42, 8145 (1990).
- [45] Z.-F. Zhang and P. Ye, Compatible braidings with hopf links, multiloop, and borromean rings in (3 + 1)-dimensional spacetime, Phys. Rev. Res. 3, 023132 (2021).
- [46] Z.-F. Zhang, Q.-R. Wang, and P. Ye, Continuum field theory of three-dimensional topological orders with emergent fermions and braiding statistics, Physical Review Research 5, 043111 (2023).
- [47] Z.-F. Zhang, Q.-R. Wang, and P. Ye, Non-abelian fusion, shrinking, and quantum dimensions of abelian gauge fluxes, Physical Review B 107, 165117 (2023).
- [48] Y. Huang, Z.-F. Zhang, and P. Ye, Diagrammatic Representa-

tions of Higher-Dimensional Topological Orders, arXiv e-prints

, arXiv:2405.19077 (2024), arXiv:2405.19077 [hep-th].